AD_____

AWARD NUMBER DAMD17-94-J-4144

TITLE: An Examination of Ultrasound Measured Tissue Perfusion on Breast Cancer

PRINCIPAL INVESTIGATOR: Jeffrey Brian Fowlkes, Ph.D.

CONTRACTING ORGANIZATION: University of Michigan
Ann Arbor, Michigan 48109-1274

REPORT DATE: December 1998

TYPE OF REPORT: Final

PREPARED FOR: Commander
U.S. Army Medical Research and Materiel Command
Fort Detrick, Maryland 21702-5012

# REPORT DOCUMENTATION PAGE

*Form Approved*
*OMB No. 0704-0188*



| 1. AGENCY USE ONLY *(Leave blank)* | 2. REPORT DATE | 3. REPORT TYPE AND DATES COVERED |
|---|---|---|
| | December 1998 | Final (1 Jun 94 - 30 Nov 98) |

**4. TITLE AND SUBTITLE**
An Examination of Ultrasound Measured Tissue Perfusion on Breast Cancer

**5. FUNDING NUMBERS**
DAMD17-94-J-4144

**6. AUTHOR(S)**
Jeffrey Brian Fowlkes, Ph.D.

**7. PERFORMING ORGANIZATION NAME(S) AND ADDRESS(ES)**
University of Michigan
Ann Arbor, Michigan 48109-1274

**8. PERFORMING ORGANIZATION REPORT NUMBER**

**9. SPONSORING / MONITORING AGENCY NAME(S) AND ADDRESS(ES)**
U.S. Army Medical Research and Materiel Command
Fort Detrick, Maryland 21702-5012

**10. SPONSORING / MONITORING AGENCY REPORT NUMBER**

**11. SUPPLEMENTARY NOTES**

**12a. DISTRIBUTION / AVAILABILITY STATEMENT**
Approved for Public Release; Distribution Unlimited

**12b. DISTRIBUTION CODE**

**13. ABSTRACT** *(Maximum 200 words)*

Mammography has proven reliable as a screening tool for breast cancer. However, its specificity may be as low as 10% as evidenced by the number of biopsies recommended compared to the number of cancers. This research was designed to develop measurement techniques for tissue perfusion including ultrasound contrast agent interruption and decorrelation techniques.

*Contrast interruption* allows control of contrast agent flow in selected vessels and is used in conjunction with common ultrasound imaging methods that measure contrast agent signal levels dynamically or statically. The technique provides temporally sharp boluses not achievable by IV administration and durations similar to arterial administration without catheterization. These are important attributes for tissue perfusion measurements by indicator-dilution techniques. The technique can also be used to eliminate the flow of contrast agents in selected vessels to demonstrate the vascular supply for specific tissues. *Contrast decorrelation* measures motion of contrast through the ultrasound beam by examining the gradual loss of speckle coherence. The technique directly estimates a mean transit time, and at least in preliminary studies, appears to be quite angle independent. With certain modifications, the technique may directly yield perfusion in a real-time imaging application of flow in ultrasound accessible tissues.

**14. SUBJECT TERMS**
Breast Cancer, Ultrasound, Perfusion, Flow, 3-dimensional

**15. NUMBER OF PAGES**
37

**16. PRICE CODE**

| 17. SECURITY CLASSIFICATION OF REPORT | 18. SECURITY CLASSIFICATION OF THIS PAGE | 19. SECURITY CLASSIFICATION OF ABSTRACT | 20. LIMITATION OF ABSTRACT |
|---|---|---|---|
| Unclassified | Unclassified | Unclassified | Unlimited |

FOREWORD

Opinions, interpretations, conclusions and recommendations are those of the author and are not necessarily endorsed by the U.S. Army.

____ Where copyrighted material is quoted, permission has been obtained to use such material.

____ Where material from documents designated for limited distribution is quoted, permission has been obtained to use the material.

X Citations of commercial organizations and trade names in this report do not constitute an official Department of Army endorsement or approval of the products or services of these organizations.

X In conducting research using animals, the investigator(s) adhered to the "Guide for the Care and Use of Laboratory Animals," prepared by the Committee on Care and Use of Laboratory Animals of the Institute of Laboratory Resources, National Research Council (NIH Publication No. 86-23, Revised 1985).

X For the protection of human subjects, the investigator(s) adhered to policies of applicable Federal Law 45 CFR 46.

____ In conducting research utilizing recombinant DNA technology, the investigator(s) adhered to current guidelines promulgated by the National Institutes of Health.

____ In the conduct of research utilizing recombinant DNA, the investigator(s) adhered to the NIH Guidelines for Research Involving Recombinant DNA Molecules.

____ In the conduct of research involving hazardous organisms, the investigator(s) adhered to the CDC-NIH Guide for Biosafety in Microbiological and Biomedical Laboratories.

PI - Signature 12/20/98 Date

# A. INTRODUCTION

## A.1 Description of the Research (subject, purpose, scope)

The research conducted under this research grant was directed toward advancing flow measurement techniques that could eventually be used in conjunction with mammography to evaluate breast lesions. The role of mammography as a screening tool for breast cancer is well established but is not without its problems. The specificity of mammography for breast cancer may be as low as 10% as evidenced by the number of biopsies recommended compared to the number of cancers confirmed (Moskowitz and Gartside, 1982). In more recent investigations, specificity remains low and ultrasound is now being considered as capable of providing additional diagnostic information. Therefore, of significant health care benefit would be any methods used in conjunction with mammography that could reduce the number of biopsies required while maintaining or improving survival rates. The impact on health care costs is clearly a consideration. Adler *et al.* (1990) estimated that more than half of the mammographic screening costs for breast cancer are the result of required biopsies or excisions due to low specificity. The complications to the patient in terms of the inconvenience, pain and anxiety associated with unnecessary biopsies are perhaps equally important.

Our research concentrated on the development of two methods that we believe will have diagnostic benefit in breast cancer and other areas where quantitative blood flow is important. *Contrast interruption* allows control of contrast agent flow in selected vessels. It can be used in conjunction with common ultrasound imaging methods that measure contrast agent signal levels in dynamic (bolus production) or static (continuous, selective interruption) conditions. The technique provides temporally sharp boluses (sharp leading and trailing edges) not achievable by IV administration and durations similar to that of arterial administration without catheterization. These are important attributes in the measurement of tissue perfusion by indicator-dilution techniques. More simply the technique can be used to eliminate the flow of contrast agents in selected vessels to demonstrate the vascular supply for specific tissues. This could be used for identification of vessels for occlusive therapy. *Contrast decorrelation* measures the motion of contrast through the ultrasound beam by examining the gradual loss of speckle coherence at a given location. The technique has the property of directly estimating a mean transit time, and at least in preliminary studies, appears to be quite angle independent. With certain modifications, the technique may directly yield perfusion in a real-time imaging application of flow in ultrasound accessible tissues.

## A.2 Background of Previous Work

Doppler ultrasound has been investigated and found some utility in the detection of cancer (Burns *et al*, 1982; Minasian and Bamber, 1982; Boyd *et al*, 1983). Although the specificity has been high for cancer recognition, at 10 MHz frequencies used in these studies, the sensitivity of the technique has not and the use of other Doppler techniques have had mixed specificity and sensitivity results (Rubin *et al*, 1987; Adler *et al*, 1988; Jellins, 1988; Cosgrove *et al*, 1990; Adler *et al*, 1990). The advent of stable ultrasound contrast agents and the development of Doppler power mode imaging are clearly innovations that should improve the sensitivity of ultrasound techniques for cancer.

Abnormal accumulation of contrast during the arterial phase of contrast transit and a residual concentration of contrast agent in breast cancers has been observed with conventional angiography, but without exceptionally high specificity (Feldman *et al*, 1967; Kaushik *et al*, 1975; Sakki, 1974), with x-ray computed tomography (Chang *et al*, 1982) and with digital subtraction angiography (Flynn *et al.*, 1984). Gadolinium MRI is now looking quite positive as a means of discriminating likely breast cancers and even detecting mammographically occult malignancies (Harms, et al., 1993, Heywang-Kobrunner, et al., 1992). With the advent of ultrasound contrast, such contrast studies are beginning to be performed using real-time imaging modalities which are well-suited for

dynamic contrast studies. The desired IV administration of the agent however results in dilution of the contrast and the loss of a well-resolved bolus. If such problems can be overcome, the prospect for ultrasound contrast detection of breast cancer would be greatly improved by providing a bolus with temporal resolution adequate for indicator-dilution measurements of blood flow. Doppler power imaging has also demonstrated an improved signal to noise ratio over conventional color Doppler flow imaging. Images being made in this mode seem to indicate one can expect such a modality would improve on the sensitivity of ultrasound for small vessels. Results from clinical trials on high resolution ultrasound imaging of breast has indicated its utility in the discrimination of breast cancers. Some evidence also exists that the addition of Doppler information further improves the discrimination.

Finally, work concerning angiogenesis (Weidner *et al.*, 1991; Horak, 1992) has placed renewed emphasis on the blood flow in the region of cancerous lesions. The potential of ultrasound techniques described here to measure regional perfusion suggests that information can be derived by noninvasive means using a relatively inexpensive imaging modality.

# B. DESCRIPTION OF RESEARCH PROGRESS

## *B.1 Publications and Related Communications*

The following is a list of relevant publications during the entire project project period (June 1, 1994 to December 31, 1998) which have resulted from this work.

### B.1.1 Peer Reviewed Journal Articles

Adler RS, Rubin JM, Fowlkes JB, Carson PL, Pallister JE: Ultrasonic Estimation of Tissue Perfusion: A Stochastic Approach, Ultrasound Med. Biol., Vol. 21 (4), 493-500, 1995.

Rubin, JM, Adler RS, Fowlkes JB, Spratt S, Pallister JE, Chen JF, Carson PL: Fractional moving blood volume estimation using doppler power imaging, Radiology, 197, 183-190, 1995.

Chen J-F, Fowlkes JB, Carson PL, Rubin JM, Adler RS: Auto-correlation of Integrated Power Doppler Signals and its Application, Ultrasound Med. Biol., 22, 1053-1057, 1996.

Chen J-F, Fowlkes JB, Carson PL, Rubin JM: Determination of scan-plane motion using speckle decorrelation: theoretical considerations and initial test, Int J Imaging Syst Technol, 8, 38-44, 1996.

Rubin JM, Bude RO, Fowlkes JB, Spratt RS, Carson PL, Adler RS: Normalizing fractional moving blood volume estimates with power Doppler US: Defining a stable intravascular point with the cumulative power distribution function. Radiology, 205, 757-765, 1997.

Tuthill TA, Kruecker JF, Fowlkes JB, Carson PL, Automated 3-D US Frame Positioning Computed from Elevational Speckle Decorrelation, Radiology, 209, 575-582, 1998.

Fowlkes JB, Sirkin DW, Ivey JA, Gardner EA, Rhee RT, Rubin JM, Carson PL Transcutaneous interruption of ultrasound contrast agents for blood flow evaluation. Investigative Radiology, 33(12) 893-901 1998.

Rubin JM, Fowlkes JB, Tuthill TA, Moskalik AP, Rhee RT, Adler RS, Kazanjian S, Carson PL (1999) Decorrelation in B-mode images of contrast agent for blood flow measurements, Radiology, accepted.

### B.1.2 Patents:

Fowlkes JB, Carson PL, Moskalik A, Chen JF: Method and Apparatus for Composition and Display of Three-Dimensional Image from Two-Dimensional Ultrasound Scan Data,

Application for U.S. Letters Patent, June 15, 1995. International statement of intent, 1996, International submission, 1997.

B.1.3 Invited Presentations

Fowlkes JB, Ivey JA, Gardner EA, Rubin JM, and Carson PL: The potential for ultrasound contrast bolus production using acoustic fields: Bubble generation and manipulation 36th Annual Meeting of the Amer. Assoc. Physicists in Med., Annaheim CA, Aug., 1994, abstract.

Fowlkes JB Understanding the origins of nonlinear emissions from contrast agents, Invited lecture at the Symposium on Ultrasound and Microbubbles sponsored by the Japan Society of Ultrasound in Medicine, Sept. 27, 1996.

Fowlkes JB, Sirkin DW, Rhee R, Rubin JM, Carson PL (1997) Generation and detection of negative contrast boluses for use in blood flow studies, Invited lecture for the 2nd Thoraxcenter European Symposium on Ultrasound Contrast Imaging, Rotterdam, the Netherlands, Jan. 23-24, 1997.

Fowlkes JB (1997) Hot Topics in Medical Acoustics (Advanced Techniques in Ultrasound Contrast Agents), Invited lecture at the 133rd meeting of the Acoustical Society of America, June 15-20, 1997, J. Acoust. Soc. Am. 101 (5) pt.2, 3120.

B.1.4 Book Chapters (which included topics related to this project)

Fowlkes JB and Hwang EY, "Echo-Contrast Agents - What Are The Risks?" in Safety of Diagnostic Ultrasound, S Barnett and G Kossoff, eds. from the series Progress in Obstetric and Gynecological Sonography, A Kurjak, ed., Parthenon Publishing, UK.

B.1.5 Abstracts and Proceedings

Fowlkes JB, Ivey JA, Gardner EA, Rubin JM, and Carson PL: "New acoustical approaches to perfusion and other vascular dynamics", Presentation at 127th Meeting of the Acoustical Society of America, Cambridge, MA, June 6-10, J.Acoust. Am. 95, 2855, 1994.

Fowlkes JB, Ivey JA, Gardner EA, Rubin JM, and Carson PL: The potential for ultrasound contrast bolus production using acoustic fields: Bubble generation and manipulation 36th Annual Meeting of the Amer. Assoc. Physicists in Med., Annaheim CA, Aug., 1994, abstract.

Fowlkes JB, Gardner EA, Carson PL, Ivey JA, Rubin JM: "Acoustic Interruption of Ultrasound Contrast Agents for Blood Flow Evaluation", Procs., 39th Annual Conv. of the American Institute of Ultrasound in Medicine, San Francisco, CA, March 26-29, J. Ultras. in Med.14, S59, 1995.

Rubin JM, Ader RS, Fowlkes JB, Spratt S, Pallister JE, Chen J-F, Carson PL (1995) Fractional Moving Blood Volume Estimation Using Doppler Power Imaging, Twentieth International Symposium on Ultrasonic Imaging and Tissue Characterization, Arlington, VA, Program and Abstracts, June 7-9, 1995.

Fowlkes JB, Gardner EA, Carson PL, Ivey JA, Rubin JM Use of Contrast Interruption in Measurement of Blood Flow, Twentieth International Symposium on Ultrasonic Imaging and Tissue Characterization, June 7-9, Arlington, VA, 1995.

Loetsch R, Chen J-F, Fowlkes JB, Carson PL Measurement of Linear and Nonlinear Acoustic Properties of MRX-115 Contrast Agent, Twentieth International Symposium on Ultrasonic Imaging and Tissue Characterization, June 7-9, Arlington, VA, 1995.

Chen, JF, Fowlkes JB, Carson, PL and Moskalik: Determination of Scanhead Motion Using Decorrelation of Speckle, AAPM 37th Annual Meeting and Exhibition, Boston, MA, July 23-27, 1995.

Fowlkes JB: Progress in Perfusion and Moving Fractional Blood Volume Estimation Using Doppler Imaging. Ninth International Congress on the Ultrasonic Examination of the Breast, Indianapolis, IN, Sept. 28-October 1, 1995.

Moskalik, AP, Chen, JF, Fowlkes JB, Carson, PL: Image-Based Registration (IBaR) for Positioning Ultrasound Images in Three Dimension. J Ultra. Med: 15:S2, March, 1996.
Rubin, JM, Adler, RS, Fowlkes JB, Spratt, S, Pallister, JE, Chen, JF, Carson, PL: Fractional Moving Blood Volume Estimation Using Power Doppler Imaging. J. Ultra. Med: 15:S41, March, 1996.
Fowlkes JB, Gardner, EA, Carson, PL, Rhee, R, Rubin, JM: Transcutaneous Interruption of Contrast Agents for Blood Flow Evaluation. J. Ultra. Med.: 15:S58-S117, March, 1996.
Fowlkes JB, Sirkin DW, Rhee R, Rubin JM, Carson PL (1997) In Vivo Interruption of Contrast Agents for Temporally Short Arterial Bolus Production, (Procs., AIUM 39th Annual Conv., Mar. 17-20) J. Ultras. in Med., 16:S1, S36.
Fowlkes JB, Moskalik A, Rhee R, Rubin JM, Adler RS, Carson PL (1997) Decorrelation Imaging of Contrast Agents for Flow Detection, (Procs., AIUM 39th Annual Conv., Mar. 17-20) J. Ultras. in Med., 16:S1, S22.
Fowlkes JB, Sirkin DW, Rhee R, Rubin JM, Carson PL, Generation and Detection of negative contrast boluses for use in blood flow studies, 2nd Thoraxcenter European Symposium on Ultrasound Contrast Imaging, Rotterdam, the Netherlands, Jan. 23-24, 1997.
Fowlkes JB, Moskalik A, Rhee R, Sirkin DW, Rubin JM, Adler RS, Carson PL (1997) Ultrasonic Measures of Blood Flow Using Contrast Agents, U.S. Army Breast Cancer Research Program., Oct. 31-Nov 4. Chicago, Poster, Proceedings, I, 219-220.
Rhee R, Fowlkes JB, Rubin JM, Carson PL (1998) Disruption of Contrast Agents Using Pulsed Ultrasound, (Procs., AIUM 42nd Annual Conv., Mar. 22-25) J. Ultras. in Med., 17:S1, S97.
Tuthill TA, Fowlkes JB, Krueker JF, Rubin JM, Carson PL (1998) Elevational B-Scan Registration Using Frame-to-Frame Speckle Decorrelation, (Procs., AIUM 42nd Annual Conv., Mar. 22-25) J. Ultras. Med., 17:S1, S96.
Fowlkes JB. Ultrasound-induced effects by contrast media. (Procs., AIUM 42nd Annual Conv., Mar. 22-25, 1998) J. Ultras. Med., 17:S72.
Rhee RT, Fowlkes JB, Sirkin DW, Rubin JM, Carson PL, Disruption of Contrast Agents for Monitoring Blood Flow, Presentation at 135th Meeting of the Acoustical Society of America, Seattle, WA, June 22-26, 1998.
Krücker JF, Tuthill TA, LeCarpentier GL, Fowlkes JB, Carson PL, Image Based Calculation of Elevational B-Scan Separation, Presentation at 135th Meeting of the Acoustical Society of America, Seattle, WA, June 22-26, 1998.
Rubin JM, Fowlkes JB, Tuthill TA, et al. Decorrelation flow measurements in rabbit kidneys using ultrasound contrast agents Radiology 209P: 190-190 Suppl 1998
Rhee RT, Fowlkes JB, Rubin JM, et al. Positive contrast agent bolus using a contact scanning technique Radiology 209P: 191-191 Suppl 1998
Tuthill TA, Krucker JF, Fowlkes JB, et al. Automated three-dimensional US frame positioning computed from elevational speckle decorrelation Radiology 209: (2) 575-582 1998.

## *B.2 Project Personnel Listing*

The following is a list of personnel that were supported by this research project.

PII Redacted

| Name |
|---|
| [redacted] |
| ADLER RONALD S |
| CARSON PAUL L |
| CHEN JIAN-FENG |
| DAS RAJEEB L |
| FOWLKES J BRIAN |

PII Redacted

[redacted] LONGINO MARC ALAN
[redacted] RUBIN JONATHAN M
[redacted] SIRKIN DAVID W
[redacted] TUTHILL THERESA A

## B.3 Ultrasonic Manipulation of Contrast Agents

Our research has been extremely successful at initially demonstrating the concept of controlling the flow of ultrasound contrast agent by the transcutaneous application of ultrasound. There has been an evolution of the concept, described below, that has taken this research to within possible clinical application. The research effort has yielded a simple yet elegant technique where the commonly used indicator-dilution techniques for perfusion measurement may be possible in the not-too-distant future.

## B.4 Production of the Negative Bolus

The elimination of contrast agent flow has been accomplished in a series of experiments that are described in detail in Fowlkes et al (1998). These experiments use a waterpath standoff system and high intensity ultrasound to produce a negative bolus in an vessel. The bolus was then detected at a down stream location. The experiments were conducted as follows.

### B.4.1 Methods

Experiments were performed in adult female New Zealand albino rabbits, 2.0-3.7 kg, anesthetized with xylazine (Rompun) (10 mg/kg s.c.) and ketamine (50 mg/kg i.m.). Supplemental doses of ketamine were administered i.v. through an ear vein catheter. The rabbit was placed supine on a heating pad with temperature maintained at 36.5 to 37.5 °C. A thin plastic bag supported around the opening by a 30.5-cm diameter plastic cylinder was placed over the rabbit's abdomen and inner thigh and coupled to the skin with degassed coupling gel. The tank is then filled with 35 °C degassed deionized water. The water in this coupling bath was continuously replaced by means of a pump and a drain with water from a tank equipped with a degasser (Kaiser *et al.*, 1996) and a heating coil.

MRX115 contrast agent (ImaR$_X$ Pharmaceutical Corp., Tucson, AZ) was administered through the ear vein catheter, either as a 10 µl/kg bolus (approximately $10^6$ bubbles/kg) or diluted to 4% (vol./vol.) in saline and infused for up to 12.5 min at 0.4 ml/min using a syringe pump. This transpulmonary agent is a lipid-shelled gas bubble containing perfluoropropane.

A two element annular array (Etalon Inc. Lebanon, IN) with a 10 mm inner element diameter (5 MHz) and a concentric 67 mm outer element diameter (1.8 MHz) (both of proprietary PZT material) was used in these experiments. The endocavitary probe was a 7 MHz convex linear array and was fixed to the high-intensity transducer in order to position the focal point. A plastic pointer was temporarily placed at the focal point of the transducer so that this position could be marked on the monitor screen of the Diasonics scanner (Ivey *et al.*, 1995). A second scanhead (40 mm, 10 MHz linear array) was placed directly against the outer thigh just above the knee. An artery was located in the outer thigh and the Doppler spectrum was recorded from it. Spectral data of 4 or 8 seconds duration were stored on an internal hard disk of the scanner for later processing. The overall experimental arrangement is diagrammed in Fig. 1 including the associated electronics. This system has been used in numerous subsequent experiments.

In one of the early animal experiments, the right thigh of the animal contained a VX2 tumor to demonstrate that the contrast interruption could be observed in a tumor model. Rabbit VX2 carcinoma is an anaplastic tumor derived from a malignant transformation of a virally induced papilloma of the domestic rabbit. The tumor grew three weeks before the ultrasound procedures described above. Doppler spectra were obtained from vessels in the tumor periphery.

Gross examination was performed on the tissue at the site of contrast interruption. This revealed no obvious effects. The experiments reported herein were conducted in an ethical and humane fashion and experimental design was approved by the University of Michigan's Committee on Use and Care of Animals in accordance with U.S. government guidelines.

### B.4.2 Data analysis

Each spectrum from the Diasonics (example shown in Fig. 2A) was integrated over frequencies to give a time record of Doppler signal power which is similar to the information in power Doppler imaging (Rubin *et al.* 1994; 1995) (Fig. 2B). Since the pixel intensities in the Diasonics spectra are on a nonlinear scale ("compressed" data) in order to enhance the ability of a user to discriminate intensity levels, these values were linearized prior to integration.

A new technique of data analysis was developed as part of this effort. A cumulative power Doppler curve (integral over time of the power Doppler record) was generated and then fit with three connected line segments (the modeled integral of a notch or rectangular negative pulse) (Figs. 2C, 3). The program was provided with a first approximation of the function consisting of three connected line segments. The computer program was provided with the beginning and end points of the data to fit (the entire 4- or 8-second saved data set or else a smaller region around the apparent interruption of contrast was fit) as well as starting values of 5 parameters: the slopes of the 3 line segments, $m_1$, $m_2$, $m_3$, and the x-coordinates of the two end points of the middle line segment, p and q. These 5 parameters were adjusted by the computer to get a local least squares fit (see Figs. 2C, 3). The parameters $m_1$ and $m_3$, which represent the average Doppler power before and after the interruption respectively (Fig. 3), were allowed to take values that differed from each other. This allowed for better fits in some instances in which the average enhancement from the contrast agent changed somewhat over the recording time segment. The left-most line segment was anchored to the curve at the left end of the region to be fit, obviating the need for a y-intercept as a 6th fitting parameter.

The following quantities were defined by the five fitting parameters $m_1$, $m_2$, $m_3$, p, and q: The baseline is the average of $m_1$ and $m_2$. The *fractional reduction* in the Doppler power signal is the reduction divided by the baseline, where the reduction is the difference between $m_2$ and the baseline (Fig. 3). The *interruption delay* is the time between onset of the high intensity ultrasound pulse and p. The *interruption duration* is the time from p to q. The *total input* is the product of the amplifier pulse duration and voltage, and the *total effect* is the product of the fractional reduction and the interruption duration.

### B.4.3 Results

*Measurements in Femoral Artery*

In all rabbits, ultrasound pulses of sufficient amplitude focused at the femoral artery near where it enters the thigh from the abdominal region caused transient decreases of MRX115 contrast agent enhancement in a distal artery near the lateral surface of the thigh just above the knee. These decreases were discernible in the Doppler spectra on the monitor screen of the Diasonics ultrasound scanner (Fig. 2A). Figure 2B shows the corresponding integrated Doppler power for the spectrum of Fig. 2A. In the integrated spectrum of the linearized Doppler power, the large decrease in the signal power due to the negative bolus passage is easily seen at 1-2 seconds (time is reference to the firing of the interruption burst at time =0). The integrated Doppler power has numerous spikes

due to the pulsatile nature of the arterial flow and noise. A cumulative power over time (Fig. 2C) yields a much smoother curve that facilitates quantification (see Methods). The cumulative Doppler power also shows the expected gradual increase in accumulated signal prior to the arrival of the negative bolus and a sudden change in slope as the bolus passes. Our quantitative analysis of the fitted results such as that of Fig. 2C yielded fractional reductions (defined in Methods) as large as 90%. Measurements in 2 of the rabbits indicated that the contrast agent increased the integrated power Doppler signal by roughly a factor of 10 to 20 over blood without contrast agent. Therefore further reductions beyond 90% may not have been possible because the residual signal level was probably that of blood alone, without agent, in our most effective trials.

The duration of the reduction (bolus duration) and fractional reduction of Doppler power at the downstream monitoring site generally increased with increasing duration and amplitude of the high-intensity ultrasound pulse (Figs. 4, 5, 6). There was some variability from one rabbit experiment to another in the degree of interruption and ultrasound amplitudes required as indicated in Figure 5. In Fig. 5A, the results for five of the animals are summarized for a 1-second ultrasonic burst. The fractional reduction increased with increasing acoustic output in some rabbits but not in others. In the latter case, maximal reduction was achieved by even the lowest intensities used, approximately 3 W/cm$^2$. There was considerable variability in the fractional reduction perhaps due to targeting errors of the narrow beam and the potential for not applying a uniform amplitude across the artery. The minimum $I_{SPPA}$ values needed to produce an average fractional reduction of at least 0.5 for an ultrasound pulse of 0.25 s duration ranged from 2.3 and 360 W/cm$^2$ among 4 rabbits (the fifth died, apparently from administration of supplemental ketamine, after only two pulses of ultrasound had been delivered). However, as will be indicated in the discussion below, pulsed ultrasound has produced contrast interruption at considerably lower acoustic amplitudes.

There was a tendency for interruption durations to be substantially longer than burst durations, particularly when the burst durations were short (Figs. 4B, 5D). When the interruption duration was short, the delay time tended to be shorter, indicating that the algorithm was choosing point p (refer to Fig. 3) to be farther to the left in those cases, but the position of point q was not changing substantially. This was possibly an artifact of the curve fitting procedure but there also seemed to be a limit to how short an interruption could be made. The bursts used to make the interruptions in the VX2 carcinoma experiment (as short as 40 cycles, or ~ 20 μs) were very much shorter than the interruptions they produced (1 cardiac cycle, or about 0.3 s) (See below). This result is similar to those of the study by Ivey *et al.* [9] in which high intensity fields were used to produce cavitation bubbles for ultrasound contrast; short acoustic bursts produced contrast enhancement downstream which was at least one cardiac cycle in duration.

A trend for increasing duration of the negative bolus (interruption duration) may exist when increasing the peak negative pressure (PNP) of the applied bursts (Fig. 5B). This might be caused by a longer length of the artery being exposed to amplitudes above that necessary for bubble destruction. Holding PNP constant, the fractional reduction was only marginally greater for longer burst durations (Fig. 5C).

The delays among and within rabbit experiments did not seem to be correlated with cardiac pulse rate. The cardiac pulse rate was typically about 195 bpm, and varied substantially over the course of an experiment in only one rabbit. There was no consistent indication of contrast agent enhancement after the interruption ($m_3$ was not consistently greater than $m_1$).

*Measurements in VX2 Carcinoma*

Figure 6 shows the results for the demonstration of contrast interruption in the VX2 carcinoma. As indicated above ultrasound was applied to the femoral artery to control the flow of contrast agent downstream. Figure 6A is a spectral Doppler taken from the peripheral vasculature of the tumor. The spectrum shows the interruption (noted as the reduction in signal brightness) following the application of a 250 ms ultrasound burst. The bright vertical streak seen in the spectrum is caused by the interference of the interruption pulse with the imaging system. Note the

reduction of Doppler signal that appears near the center of the time record. Figure 6B shows the Doppler spectrum for a substantially shorter burst (~40 μs). As indicated above the duration of the contrast interruption is still approximately one cardiac cycle.

## B.5 Use of Low intensity Pulsed Ultrasound for Interruption

One of the most significant issues facing successful contrast manipulation *in vivo* was the acoustic intensity required to produce reliable interruptions. In our previous experimentation, we used acoustic fields comprised of long bursts of continuous wave (CW) ultrasound. In order to obtain substantial interruption of the contrast agent flows, the acoustic intensity required reached a level where significant bioeffects due to heating could be expected. Therefore, we concentrated on methods to reduce the acoustic intensity. The results of our initial *ex vivo* efforts reduced the acoustic field to a level that is **within the FDA limits for diagnostic ultrasound.** This is very important to the long-term clinical viability of any of the interruption techniques.

Experiments have been performed for a variety of pulse parameters and the results indicate that a wide range of values will provide interruptions in the flow of contrast agent. Figures 7 and 8 show some of the results of these experiments. In Figure 7, the duration of the contrast interruption is plotted as a function of the peak rarefactional pressure in the applied waveform. Figure 7A shows the results when a 2.0 second duration burst sequence is applied which results in approximately the same interruption duration. There is a slight trend toward longer interruptions at the higher acoustic pressures. The interruption is quite reproducible under these conditions where the error bars represent the standard error of the mean. Note also that very little dependence on PRF is seen in the almost one order of magnitude range tested. Figure 7B shows the results for a variety of burst sequence durations (0.5, 1.0, 2.0 sec). In all cases the duration of the interruption measured downstream is slightly higher than the burst sequence. However, in each case there was very little PRF or acoustic amplitude dependence over the range of values tested.

The degree to which the contrast agent was disrupted by the field did vary with some acoustic parameters. As shown in Figure 8, the amount of signal reduction (meaning the ratio of the integrated Doppler signal averaged during the bolus passage to that measure prior to the interruption) was affected by the amplitude of the acoustic field. Figure 8A shows the result for a 1.0 sec burst sequence duration where it is noted that signal reduction increases with increasing acoustic pressure. Figure 8B shows the result for a 2.0 sec burst sequence in which the reduction effect appears to saturate at the higher amplitudes. Although the rate at which pulses are being applied is the same as that for Figure 8A, the degree to which the contrast agent can be disrupted is greater as the duration of the applied field increases. This change for shorter burst sequences results from the finite time for the contrast signal amplitude to increase and decrease in response to the application and elimination of the interruption field upstream. The onset of the negative bolus is not instantaneous such that the slope of the leading and trailing edge of the bolus is dependent on the acoustic amplitude applied. When averaged over the duration of the bolus, the contributions from these edges become a greater fraction of the whole bolus for short interruptions and therefore the average signal reduction is not as great. It remains the case that higher amplitudes are desirable since these will produce sharper edges to the interruption bolus and thus greater temporal resolution for flow measurements. The fact that there is little PRF dependence would imply that the contrast agent is being disrupted by the first bursts it encounters. Therefore the PRF will probably become important as the velocity of the flow increases because the requirement will be that all bubbles flowing into the focal zone must be destroyed and the faster these move into the beam, the faster bursts must be applied.

## B.6 Production of Positive Contrast Boluses

The previous results demonstrated that a pulsed multi-cycle toneburst yielded equivalent interruption efficacy as the CW high power output. With this knowledge, the negative bolus

experimental setup was modified such that a 10 or 20 cycle tone burst pulse at the resonant frequency of the interruption transducer was applied at a pulse repetition frequency (PRF) of 0.75 to 6.0 kHz. It has subsequently been determine that significantly lower amplitudes are required with pulsed ultrasound to disrupt the contrast agent. Therefore, a new *in vivo* applicator was developed that allowed direct coupling to the skin with imaging feedback. Figure 9 shows the interruption transducer (a single element, 19- mm diameter, planar transducer) attached to the Diasonics linear array used to target blood vessels. The benefit of this change was that a contact scanning technique could be applied directly, without the need for an external water path standoff. It should be noted that the interruption can be performed with the spectral Doppler or M-mode output of an ordinary ultrasound scanner thus eliminating the need for the additional transducer used here to provide a simple field that could be calibrated more easily.

A series of experiments were then performed in rabbits to demonstrate the systems efficacy in contrast interruption. Contrast agent (MRX 115, Ima$R_x$ Pharmaceuticals Corp., Tucson AZ) was administered through the ear vein catheter, either as a 10 µl/kg bolus (approximately $10^6$ bubbles/kg) using a Hamilton syringe or diluted into 10 ml of saline and infused at 1 ml/min using a syringe pump (Model 22, Harvard Apparatus South Natick, MA). Ultrasound was applied to either the femoral artery or the aorta while monitoring the vasculature downstream. In the case of the aorta, the Doppler information (power mode, color flow, and pulsed Doppler) was recorded in the renal cortex. The system has performed well in these trials, producing short periods of interruption (0.5-2.0 sec) for sharp negative boluses in the femoral artery and aorta. More recently extended interruptions in the aorta have been applied that were sufficiently long to allow contrast agent to clear the kidney, and when the sound field was turned off momentarily, a bolus of contrast was released. Figure 10 are power Doppler images of the kidney taken during the continuous interruption in the aorta (left) and at the peak of the signal due to the release of a contrast bolus. The signal increase is as much as 30 dB using this fundamental (non-harmonic) imaging mode.

Spectral Doppler data recorded during the bolus passage reveals the temporal duration of the bolus. Figure 11 shows the total Doppler power (left) and cumulative power (right) as functions of time during the passage. The Doppler spectrum was integrated over to give a time record of Doppler signal power which is similar to the information in power Doppler imaging (Rubin et al, 1994; 1995) (Fig. 11 left). Note the rapid rise and fall of signal power over a two-second interval, which corresponds to the duration of time the interruption field was turned off. The cumulative power Doppler curve (integral over time of the power Doppler record) (Fig. 11 right) was generated and then fit with three connected line segments (the modeled integral of a rectangular positive pulse). The program was provided with a first approximation of the function consisting of three connected line segments and could then provide automated estimates of the fractional increase in the Doppler power signal and the bolus duration. The pulsatility of the largely arterial signal is smoothed considerably over time.

## B.7 CONCLUSIONS- Contrast Interruptions

The efforts on contrast interruption have demonstrated that the technique can be applied *in vivo* to control the flow of IV injected ultrasound contrast agents to produce high temporal resolution boluses. The acoustic fields applied are within the acceptable range for diagnostic ultrasound as currently regulated by the FDA. Therefore, the techniques should be applicable to the evaluation of blood flow in the breast as in the detection of cancer. In addition, the ability of the method to select specific vessels and "turn off" the flow of agent would allow the determination of supply vessels for selected site. This might be useful in therapeutic applications where information on blood supply is important.

## *B.8 Decorrelation Techniques and Combination Blood Flow Measurements*

B.8.1 Applications in the detection of flow

### B.8.1.1 Measurements using integrated power Doppler

Initial theoretical studies on this subject using a stochastic model of speckle in blood (Adler et al., 1995), and modeling the fluctuation of the speckle intensity using the fluctuation-dissipation theorem, demonstrated a simple exponential relationship of the decorrelation rate for a first approximation. This would extrapolate directly to a mean transit time defined by the time constant of the exponential fall off. Our initial implementations of the monitor of flow by decorrelation were in flow tubes with non-pulsatile flow and blood simulating fluids (Chen *et al.*, 1996a) and relied on the fluctuations of Doppler power generated by the motion of blood through the ultrasound beam and the resulting Doppler "speckle". We have been able to show that the decorrelation rate depends on the location in the flow stream from which the measurements were taken. The flow decorrelated more rapidly in the center of the stream than near the walls thus correlating with flow velocity. We also were able to compensate somewhat for sampling size and hence sampling rate limitations in these flow tube experiments. There will be an unmeasurably high decorrelation rate when the displacement distance associated with the mean transit time of interest for the most rapid sampling is on the order of or greater than the dimensions of the pixel or sampling site at which the measurement is being made. One can easily compensate for this by effectively increasing the dimensions of the pixels in the image by summing across pixels in the orientation of interest. We were able to show this effect by successively increasing the number of pixels included in the decorrelation calculation. As one increases the number of pixels along the flow direction, the decorrelation rate successively decreased. This is exactly what one would expect, since the rate of decorrelation is normalized by the zero lag value. Hence it is always a percentage and this percentage depends of the initial value, which depends on the size sampled. Thus, one needs to know what the pixel size is to obtain an accurate flow velocity. However, if this is known, it is possible to accurately estimate almost any decorrelation rate. We showed this exact result in a flow phantom by comparing the decorrelation estimated velocity with that of spectral Doppler. By knowing the dimensions of the sample volume and the angle of the sampling site to the flow stream, we were able to obtain a very high correlation between a Doppler detected velocity and a decorrelation measured velocities from 0 to 20 mm/sec (slope = 0.91, $R^2 = 0.98$). We measured the decorrelation of the fluctuations of the integrated Doppler power in spectral Doppler sampling as scatterers moved through the sample volume. These were slow flows, but they corresponded to the limits of the flow rates that could be detected given the limits of the sample volume size available. Interestingly, this was about 50 times faster than the fastest decorrelation rate that we could measure using fluctuations in Doppler power using power Doppler. This shows why extending the sampling site is necessary for fast flows. However, speeds of 1 mm/sec which are well within the range for perfusion appear measurable using spectral Doppler. Further, given very rapid gray scale imaging rates, it suggested that it might be possible to estimate very slow decorrelation flow rates in gray scale.

By lengthening the sample volume in the direction of flow, it is possible to map the flow profile. At a mean velocity of about 5 mm/sec with sampling at near normal incidence, the profiles generated by decorrelation are very similar to those obtained with color Doppler. In this circumstance, we used an ultrasound bubble contrast agent, MRX 115. It required approximately 3 lags for the center of the flow stream to decorrelate, again due to the effective lengthening of the sample volume by summing pixels along the direction of flow. These were sampled at frame rates of 43 Hz. It is now possible to sample at frame rates of on the order of 150 Hz in gray scale. Hence, we could decrease the length of the sample by a factor of 4 or estimate velocities on the order of 1 mm/sec, which corresponds to capillary perfusion rates, using the same sampling dimensions.

**Table 1**

| Rabbit | Cortex (sec) | Central Vessels (sec) |
|---|---|---|
| 1 | .083 | .020 |
| 2 | .123 | .020 |
| 3 | .027 | .020 |
| 4 | .023 | .017 |
| 5 | .033 | .020 |

**Table 2**

| Rabbit | Mean | MaxDev | Percent MaxDev |
|---|---|---|---|
| 1 | 0.77 | 0.06 | 8% |
| 2 | 0.77 | 0.14 | 18% |
| 3 | 0.35 | 0.12 | 40% |
| 4 | 0.32 | 0.1 | 31% |
| 5 | 0.43 | 0.17 | 40% |

B.8.2 Use of B-mode imaging and contrast agent

The development of the decorrelation techniques for detecting blood flow initially relied on the detection of a Doppler shift from the moving blood. However it is known that the slowest flow of the capillary bed will not be detected in current Doppler imaging due to the limited frequency resolution and soft tissue motion. The decorrelation techniques being investigated are not restricted to measurement of Doppler signals and these results are summarized by Rubin *et al.* (1999). We have experimented with the use of contrast agent to provide the motion necessary for detection of blood flow in b-mode imaging. Using the protocol for infusion of contrast agent described above, a series of b-mode images of the rabbit kidney were obtained in the cine loop and processed to detect motion associated with the bubbles. The images were divided into 5X5 pixel ROIs and regional processed for the decorrelation in the same manner as for the image based registration described previously. The pixels contained in the ROIs in each image are converted to a 1D vector and the process repeated for each image. Each of these vectors are then combined in a 2-D vector. These data are then subsampled to determine the how many of the image ROIs will be used to compute the decorrelation of each ROI. The group of image ROIs is then analyzed to compute the correlation between successive ROIs in time, i.e. ROI#1 correlation to ROI#2, ROI#2 to ROI#3, etc. for a one step correlation value at each image location. This is referred to as the first time lag correlation. The process is repeated for two, three, etc. step correlations. Figure 12 shows the results of that process as first applied in an animal study. Fig. 12A shows the appearance of the contrast agent in the kidney in a single b-mode image. Note that the concentration of the agent for this experiment provided little b-mode enhancement although higher concentrations will. By taking the inverse of the correlation of the first time lag Fig. 12B was produced. Note the appearance of the major vessels in the kidney and the initial appearnce of the renal cortex. Fig. 12C is the result of the third lag and now the renal cortex signal has increased signficantly as sufficient time has elapsed for decorrelation of the signal from the slower moving blood. Finally Fig. 12D combines the information of all three images where static tisses are coded blue, faster flows in yellow and the slower in red (Not reproduced in color here). This technique is currently being developed further and *ex vivo* confirmation is planned to determine the limitation of the technique.

Figure 13 shows the results for flow tube experiments which compared the flow as measured with standard Doppler and decorrelation from b-mode images using contrast. The flow profile across the tube was generated by averaging the decorrelation values along the length of the tube, reducing the 2D image to a 1D profile (Fig. 13a). The profile was also estimated from the frequency shift image (Fig. 13b) for comparison. Note that the amount of decorrelation increases with successive lags although the proportion to the time difference between lags in somewhat incorrect, e.g. the peak velocity has decorrelation values of 30, 75, and 105 instead of the expected 30, 60, and 90

assuming the first value of 30 is absolute. This is probably due to increased dephasing in the central voxels as the velocity increases (see below). Note the overall appearance of the parabolic flow profile in both cases. Slow flows with mean velocity as low as 0.48 cm/sec were detected (No effort to determine the slowest detectable flow).

It is possible that the rate of decorrelation could be heavily influenced by bubble destruction, random/Brownian motion in the flow stream, or radiation force from the ultrasound transducer. We scanned a flow tube with standard outputs within FDA limits. Temporal decorrelations of the flow tube with the pump off required 14 lags for the center of the flow tube to decorrelate. This is approximately 3-4 times slower than with the pump on at the very low rate studied. This differential suggests that true flow should be resolvable using decorrelation.

We scanned six rabbits using these techniques. The rabbits were anesthetized with Ketamine and Rompun or more recently with isoflurane. After shaving the rabbit's flank, a linear array transducer, typically 9 MHz, was positioned over either the right or left kidney depending on access and fixed in place with a mechanical holding device. MRX 115 was injected into an ear vein, and images of the kidney with contrast agent in it were stored in a cine loop at 30 Hz. Decorrelation images were generated. The decorrelation times of the central/hilar vessels and the renal cortex were compared (Table 1). The times displayed are the 50% correlation times, i.e. the higher the time, the slower the transit time. The difference between the cortex and the central vessels is significant at $p<0.05$ (two tailed t-test).

In addition, in order to evaluate the angle independence of decorrelation, we used the rabbit kidney as a flow model. The cortical blood flow in the kidney is well known to be normal to the renal capsule. Thus, when using a linear array scan head, the kidney acts a directional flow phantom with angles from zero to $2\pi$. With the scanhead along the spinal muscles of the back, the flow in the mid-pole of the kidney would be at zero degrees, while the upper and lower poles are at $\pm\pi/2$. The Doppler profile across the kidney should approximate a parabola with the highest frequency shifts in the mid-pole and zeros at the upper and lower poles. For comparison with decorrelation, we segmented out the cortex of the kidney using morphological operators. Then the sections of the cortex were segmented into pixel-wide columns defined perpendicular to the face of the scanhead. The mean first lag decorrelation rates in these columns was then measured along with the maximum deviation from the mean for the last five rabbits. These are displayed as residual first lag correlations, the higher correlation the slower the decorrelation rate (Table 2).

Figure 14 shows the residual first lag correlation in each column across the kidney. The decorrelation could be taken to be 1-correlation, and hence again, the higher the correlation value, the slower the decorrelation. Note that the maximum deviation is relatively small, particularly when compared to what would be expected with Doppler. For example, at 60°, one would expect a 50% deviation with Doppler from the peak frequency shift on the average; < 40% was detected with decorrelation.

Soft tissue motion will cause speckle to decorrelate. Advantages of decorrelation flow measurements are that one can make the measurements using continuous infusions of contrast agent, and by changing the sample size, it is possible to focus in on any given perfusion rate. For example, a very small sample volume will permit slowly moving material to decorrelate relatively rapidly, which in the limit could be much faster or certainly on the order of any limiting soft tissue motion. Thus, one would like to be certain that there is no significant soft tissue motion during a breath hold. In this regard, we scanned the liver and kidney of a normal volunteer with a heart rate of 60 beats per minute during breath holding. If soft tissue motion was not a factor, the speckle in the imaged tissue should never decorrelate. Within the limits of this measurement, this is true. It should be noted that since the decorrelation sample size can be controlled, the length of time of the breath hold could be very short, on the order of a few heartbeats. This should be tolerable for even relatively sick patients.

## B.9 Applications in image-based registration (IBaR) for 3D ultrasound

One of the significant advances initiated by this research was the use of the decorrelation idea in another area that impacts the future of how 3D ultrasound. As was indicated in our original proposal, this work was being performed in conjunction with that of Dr. Paul Carson on 3D breast imaging. Even though 3D imaging was not a specific part of this grant, the idea was to utilize the same data acquisition system so comparison could be made between techniques. In the course of conversations concerning the difficulties associated with breast scanning, it was suggested that the elimination of encoding hardware used to track the position of the scanhead during 3D scanning would be desirable and helpful in terms of examining images acquired from a variety of scanners. It was suggested that one might be able to use the decorrelation of signal in the elevational direction to determine the separation between slices which were obtained using a manual scan. The following is a description of the progress made in this area. This work led to a patent application in the US and several other countries. Unknown to us a diagnostic ultrasound manufacturer also filed a patent slightly after ours but which subsequently issued first in the US. International patent rights were retained by the University of Michigan as our filing date was the earliest. At least two ultrasound manufacturers are now using some form of image-based registration for 3D ultrasound.

The approach being taken by most ultrasound companies is to build a (usually hand-held) motorized scan head specifically for 3-D imaging. This approach has a disadvantage of high cost, low reliability and limitation on the number of scan heads available for 3-D. Often coupling paths are employed with their inherent attenuation and reverberation problems. Also, the scan rate for optimal color flow imaging is a complex function of all the Doppler time constants, frame rate and the particular vascular signal levels. In regular imaging with a given scan head, the operator or observing radiologist might want to capture in 3-D images observed with a particular scanner using an arcing or linear sweep. If relative 3-D image position can be obtained by processing the series of images or data used to produce the images, a great new flexibility and efficiency will be achieve. Major 3-D capabilities will only be required on a central workstation that can record a single series of images and display them in their proper position in a stacked slice 3-D display. The radiologist, technologist at the scanner, or other trained observer will view the slices sequentially in their proper position on the display. They will select the most appropriate 2, 3 or 4-D display method and views to demonstrate the noted information in the most informative way for surgeons and other referring physicians or to obtain the desired quantitative measurements.

Correlation techniques have been used extensively to estimate tissue motion in applications such as blood flow (Adler, Rubin et al. 1995) and imaging tissue elastic properties (Adler, Rubin et al. 1990; Ophir, Cespedes et al. 1991; Chen, Jenkins et al. 1992; O'Donnell, Skovoroda et al. 1994). Some commercial ultrasound systems now use correlative algorithms for their color flow imaging rather than various forms of Doppler processing. We use correlation to perform the opposite task namely assume the tissue to be stationary and track the movement of the transducer. Trahey *et al* (1986) used correlation of speckle to determine the amount of lateral translation of a phased array required to achieve statistically independent information for speckle reduction by image compounding. Their experimental results show correlation curves as a function of translation distance which are smoothly varying, suggesting that measuring the rate of decorrelation and knowing the point spread function for the aperture, one can use the same speckle statistics to estimate the actual transducer motion. The correlation techniques which we have developed provide the mechanism for slice positioning and involve the adaptation of some software already developed.

In order to test the concept of image-based slice positioning, images of a rather inhomogeneous contrast detail phantom were made. In all cases the images were post-processing in a modular code under the AVS software package of Advanced Visualization Systems. A full description of the mathematical process is given by Chen *et al.* (1996). Images were collected from an ultrasound scanner and read into the workstation memory. The RGB images are then processed to select one channel for B-mode and then the 3-D data set is sliced and a single 2-D plane displayed to select regions of interest (ROIs) to be processed for determining the slice separation. The pixels

contained in the ROI in each image are converted to a 1D vector and the process repeated for each image. Each of these vectors are then combined in a 2-D vector. These data are then subsampled to determine the how many of the image ROIs will be used to compute the position of each image. The group of image ROIs is then analyzed to compute the correlation between successive ROIs, i.e. ROI#1 correlation to ROI#2, ROI#2 to ROI#3, etc. for a one step correlation value. The process is repeated for two, three, etc. step correlations. For the hand-scanned images, ROIs from groups of ten images were used to determine the slice separation for the center two slices, e.g., to position image 6 with respect to 5 use information from images 0-9, for image 7 after 6 use image 1-10, etc. This does assume a piece-wise smooth motion for the scanhead, which should be achievable and is necessary for any good continuous power mode imaging. In each case, the correlation curve was fit using a least squares approach to the Gaussian function giving the relationship between step size, point spread function and correlation value. This information is then used to position the images appropriately in space for further display.

Two sets of images were obtained in the initial trial. A measured correlation curve was first determined for mechanical stepping with the breast scanner using a 3.5 MHz curved linear array. Using several regions of interest at the same depth range and a least squares method for a Gaussian curve-fitting, the step size was estimated for several regions of interest to be $\delta y = 0.17 \pm 0.02$ mm, compared to the actual step size used of 0.175 mm. In this case the decorrelation curve was measured across a number of images where it could be assumed that the step size was constant for the mechanical stepping. A hand scan was then performed where images at 32 fps were stored in a 120 frame cine loop. Results given in Fig. 15 show that the appearance of the echogenic cone is not very different for this short scan when using either an equal slice separation assuming uniform hand scanning rate or that calculated using the image decorrelation rate. However, the lower graphs illustrate the decorrelation does track smoothly the nonuniform motion of the slow, hand scanning currently used for 3-D power mode imaging. Black stripes in the subtraction image correspond to zeros in the integral displacement error of the uniform stepping as plotted in the graph on the right.

These techniques can be used to correct positioning errors for hand-scanned image acquisitions in the breast. This could have an important impact in the research being performed here since regional perfusion measurements will rely on know the position of the scanhead when combining Doppler power and velocity information together as an estimate of perfusion. The image-based slice positioning techniques will allow more examinations to be performed in some of the more interesting cases, i.e. the smaller dense breast which is a particular difficulty in mammography. As a demonstration of the use in the breast, experiments similar to those in the phantom were performed. Results are presented in Figure 16. In this case, the breast was scanned using a motorized positioning system for 3D ultrasound. The scanhead was translated in the elevational direction across a plastic membrane in an immobilization system similar to that used in mammography for stabilizing the breast against motion. In the upper portion of the figure are two curves. The thinner of these two refers to the results of processing the series of images using strictly the methods described above. However, it is possible for the breast to move during the procedure so an additional measurement was made. For each pair of adjacent images, the images were shifted in the axial and lateral directions to maximize the correlation. The result of the measurement is presented as the curve at the bottom of the figure. With this information, the positions of each image was adjusted and the IBaR processed repeated and the results presented as the thicker of the upper curves. Note the reduction of the variation in the slice variation. The overall results were as foolows:

In Breast : Calculated $0.22 \pm 0.03$ mm

Actual 0.20 mm spacing based on motorized positioning

After Lat/Ax Correct. $0.20 \pm 0.02$ mm

Actually, one can expect that there was indeed motion during this process so the slice positioning determine by both the in-plane correlation procedure and the decorrelation measurement may actually be more accurate that relying on the assumption of no motion and mechanical positioning. This technique has been tested further under other funding and some of the results are contained in Tuthill *et al.* (1998).

### *B.10 CONCLUSIONS-Decorrelation*

The decorrelation methods developed under this research have indicated potential for monitoring both blood flow and the position of images for 3D ultrasound. Each of these have important implications for breast imaging. Flow variations are expected to exist within and around tumors in the breast. The decorrelation of contrast agent flow may provide more information than that found with Doppler and quantitative flow measures not possible due to angle dependences. In combination with a fractional blood volume measurement (Rubin *et al.*, 1995), this method may approach a perfusion measurement that is highly desirable. The elimination of position encoding hardware in 3D ultrasound will provide the opportunity for simple hand scanning to produce a more complete picture of the breast structure.

## C. REFERENCES

Adler DD, Carson PL, Rubin JM (1988) Evaluation of Doppler ultrasound flow imaging in the diagnosis of breast cancer. Procs.World Federation Ultras. in Med. and Biol., Oct. 17-21, J. Ultrasound Med, **7**, S271, abstract only.

Adler DD, Helvie MA and Ikeda DM (1990) Follow-up strategies for marginally suspicious nonpalpable breast lesions, Amer. J. Roentgenol., in press.

Adler, R. S., J. M. Rubin, et al. (1989). "Characterization of transmitted motion in fetal lung: Quantitative analysis." Med. Physics 16(3): 333-337.

Axtel LM, Asire AJ, and Meyer MH (eds) (1976) Cancer patient survival. Report #5. DHEW Pub. No. (NIH) 77-992, Bethesda MD, NCI.

Boyd J. Jellins J, Reeve TS, and Kossoff G. (1983) Doppler Examination of the Breast *in* Ultrasound Examination of the Breast. Ed, J. Jellins and P. Kobayashi, John Wiley and Sons, New York, 386.

Burns PN, Halliwell M, and Wells PNT (1982) Ultrasonic Doppler studies of the breast. Ultrasound in Med. and Biol. 8, 127.

Chang CHJ et al (1982) Computed tomographic mammography using a conventional bodyscanner. Am. J. Reont. 138, 553.

Chen, E. (1992). Uncertainty in Estimating Tissue Motion from Ultrasonic Images. Department of Electrical and Computer Engineering, University of Illinois, Urbana, IL.

Chen J-F, Fowlkes JB, Carson PL, Rubin JM, Adler RS: (1996a) Auto-correlation of Integrated Power Doppler Signals and its Application, Ultrasound Med. Biol., 22, 1053-1057.

Chen J-F, Fowlkes JB, Carson PL, Rubin JM, Adler RS: (1996b) Auto-correlation of Integrated Power Doppler Signals and its Application, Ultrasound Med. Biol., 22, 1053-1057.

Cosgrove DO, Bamber JC, Davey JB, McKinna JA and Sinnett HD (1990) Color Doppler signals from breast tumors, Work in progress. Radiology, 175-180.

Feldman F et al. (1967) Arteriography of the breast. Radiology 89, 1053.

Flynn MJ, et al. (1984) Digital Subtraction Angiography Techniques for the Evaluation of Breast Lesions. Park Press, SPIE Vol. 468, 129.

Harms, et al. (1993) MR imaging of the breast with rotating delivery of excitation off resonance: clinical experience with pathological correlation. Radiology, 187, 493-501.

Heywang-Kobrunner SH, Haustein J, Beck R, et al. (1992) Contrast -enhanced MR imaging of the breast: influence of dose of Gd-DTPA. Radiology, 185(P): 245.

Horak ER, Leek R, Klenk N, LeJeune S, Smith K, et al. (1992) Angiogenesis, Assessed by Platelet/Endothelial Cell Adhesion Molecule Antibodies, as an indicator of Node Metastasese End Survival in Breast Cancer, Lancet, 340, 1120-1124.

Ivey JA, Gardner EA, Fowlkes JB, Rubin JM, Carson PL. Acoustic generation of intra-arterial contrast boluses. Ultrasound Med Biol 1995;21:757-767.

Jellins J (1988) Combining imaging and vascularity assessment of breast lesions, Ultras. Med. & Biol., 14, Sup 1, 121-130.

Kaiser AR, Cain CA, Hwang EY, Fowlkes JB. A Cost Effective Degassing System for Use in Ultrasonic Measurements: The Multiple Pinhole Degassing System. J. Acoust. Soc. Am. 1996;99(6):3857-3859.

Kaushik SP, Desle BY, Sodhi JS (1975) Breast angiography and clinico-pathological correlation in breast tumours. Indian J. Cancer, 367.

Minasian H and Bamber J (1982) A preliminary assessment of an ultrasonic Doppler method for the study of blood flow in human breast cancer. Ultrasound in Med. and Biol. 8, 357.

Moskowitz M, and Gartside PS (1982) Evidence of breast cancer mortality reduction, aggressive screening in women under age 50. AJR 138, 911-916.

O'Donnell, M., A. Skovoroda, et al. (1994). "Internal displacement and strain imaging using ultrasound speckle tracking." IEEE Trans. Ultras. Ferroelect. Freq. Control 41: 314-325.

Ophir, J., I. Cespedes, et al. (1991). "Elastography: a quantitative method for imaging the elasticity of biological tissues." Ultrasonic Imag. 13: 111-134.

Rubin JM, Carson PL, Zlotecki RA, and Ensminger WD (1987) Visualization of tumor vascularity in a rabbit VX2 carcinoma by Doppler flow mapping. J. Ultrasound Med. 6, 113.

Rubin JM, Bude RO, Carson PL, Bree RL, Adler RS. (1994) Power Doppler US: a potentially useful alternative to mean frequency-based color Doppler US. Radiology 90:853-856.

Rubin JM, Adler RS, Fowlkes JB, Spratt S, Pallister JE, Chen J-F, Carson PL. (1995) Fractional moving blood volume: estimation with power Doppler US. Radiology 197:183-190.

Rubin JM, Fowlkes JB, Tuthill TA, Moskalik AP, Rhee RT, Adler RS, Kazanjian S, Carson PL (1999) Decorrelation in B-mode images of contrast agent for blood flow measurements, Radiology, accepted.

Sakki S (1974) Angiography of the female breast. Ann. Clin. Res. 6, Suppl. 12, 1.

Trahey, G., E (1986). "Speckle Pattern Correlation with Lateral Aperture Translation: Experimental Results and Implications for Spatial Compounding." IEEE Trans. on Ultra. Ferroelectrics, Frequency Control UFFC-33(3): 257-264.

Tuthill TA, Kruecker JF, Fowlkes JB, Carson PL (1998) Automated 3-D US Frame Positioning Computed from Elevational Speckle Decorrelation, Radiology, 209, 575-582.

Weidner N, Semple JP, Welch WR, Folkman J (1991) Tumor Angiogenesis and Metastasis Correlation in Invasive Breast Carcinoma, The New England Journal of Medicine, Vol. 324, No. 1.

# D. FIGURE CAPTIONS

Figure 1. Diagram of the experimental set-up for contrast interruption experiments.

Figure 2. Sample of a single interruption as it appears in the femoral artery downstream from the site where the acoustic interruption is applied: A) Doppler spectrum image from Diasonics scanner. The white arrow indicates the location where the negative bolus appears. Note the reduced brightness at this location. B) The same data presented in A but integrated over frequency at each time point. There is a considerable reduction in the integrated Doppler power as the bolus passes at the 1 second point (1 second after the interruption field was applied upstream), C. Time integration of the data in B (cumulative integrated power Doppler) with 3-line-segment fit (see text and Fig. 3) showing a reduced slope for the region in which the negative bolus passes.

Figure 3. Diagram indicating how the integrated power Doppler was analyzed to quantify the interruption of contrast agent enhancement. A. An interruption in integrated power Doppler as in Fig. 2B idealized to a rectangular notch. Parameters $m_1$, $m_2$ and $m_3$ are the average Doppler power before, during and after the interruption respectively. B. The integral over time of the function in A is a 3-line-segment function that was used to fit integrals over time of interruptions in integrated Doppler power.

Figure 4. Effect of peak negative pressure and duration on downstream interruption of contrast agent. Fractional reduction (A) and interruption duration (B) taken from data from one rabbit (Rabbit 5). Each bar indicates the average of 1-5 trials.

Figure 5. Data from 5 rabbits showing the effect of peak negative pressure, with burst duration fixed at 1 s (A, B), and the effect of burst duration, with peak negative pressure fixed at approximately 2.5 MPa (C, D). Each point is an average of 2-6 trials. Error bars are standard deviations multiplied by the Gurland-Tripathi correction factors for small n.

Figure 6. Spectral Doppler waveforms taken from the experiment on VX2 carcinoma in rabbit thigh. The femoral artery was targeted upstream of the tumor and the spectral Doppler recorded in peripheral vessels of the tumor. A) The negative bolus appearing as a reduced Doppler signal (indicated by the arrow on the right) is the result of a 250 ms ultrasonic burst. Note the delay in the negative bolus arrival following ultrasonic burst (electrical interference resulting from the burst is indicated by the left arrow). B) Similar negative bolus produced by an ultrasonic burst of only ~40 μs.

Figure 7. Duration of the contrast interruption as a function of the acoustic pressure for a variety of PRFs. (A) For the case of 2.0 sec duration of burst sequence applied upstream. Error bars represent the standard error (B) For the cases of 2.0, 1.0, 0.5 sec duration.

Figure 8. Reduction in Doppler power during bolus passage as a function of the acoustic pressure for a variety of PRFs. (A) For the case of 1.0 sec duration of burst sequence applied upstream. (B) For the cases of 2.0 sec duration.

Figure 9. Apparatus for targeting and application of the interruption field using contact scanning.

Figure 10. Power mode Doppler of the kidney during contrast interruption (left) and at the peak signal following bolus release (right). Reproduced in gray-scale here.

Figure 11. Total Doppler power (left) and cumulative Doppler (right) as a function of time during the passage of a contrast bolus in kidney. The line representing the measured data (right) is jagged due to the pulsatility of the arterial supply.

Figure 12. Images of a rabbit's kidney during contast administration. A) Normal B-mode image of the kidney. Note the relative absence of contrast signal in the low concentration conditions. The image is relatively dark to demonstrate the lack of contrast agent effect. B) Lag 1 image of decorrelation where gray scale is displayed from dark to light with increasing decorrelation. Note the appearance of the larger kidney vessels and the beginning appearance of the renal cortex. C) Lag 3 image of decorrelation. The renal cortex has decorrelated further at this later point. D) Composite image where the original B-mode (A) is displayed in blue, Lag 1 (B) is green, and Lag 3 (C) is red. This figure is not reproduced in color here.

Figure 13. a) Profile of decorrelation rate averaged along the length of the flow tube. Note the appearance of the parabolic flow profile to the flow with the fastest decorrelation occurring in the middle of the tube (approximately the position of pixel 80). The amount of decorrelation is also increasing for successive lags. Decorrelation is defined here as $(1-C_N)$. b) Doppler shift profile averaged across the tube for comparison with Fig. 3a.

Figure 14. Correlation as a function of position across the kidney. Note the small devaition in value despite the wide range of flow angles interpreted.

Figure 15 - Left to right top images: 1) C-scan, longitudinal view of a cone object from a hand-scanned, 3.5 MHz, curved linear array assuming equal step size; 2) The same view with actual step size as estimated by the speckle decorrelation; 3) The subtraction between these two views (expanded horizontally). For comparison, image 1 was scaled to the same lateral size as image 2. The left graph below shows the step size change with step number as calculated from the decorrelation, while the right graph shows the integrated displacement change with step number.

Figure 16. Results of slice positioning using the IBaR method as applied in the breast. See text for a description of the method.

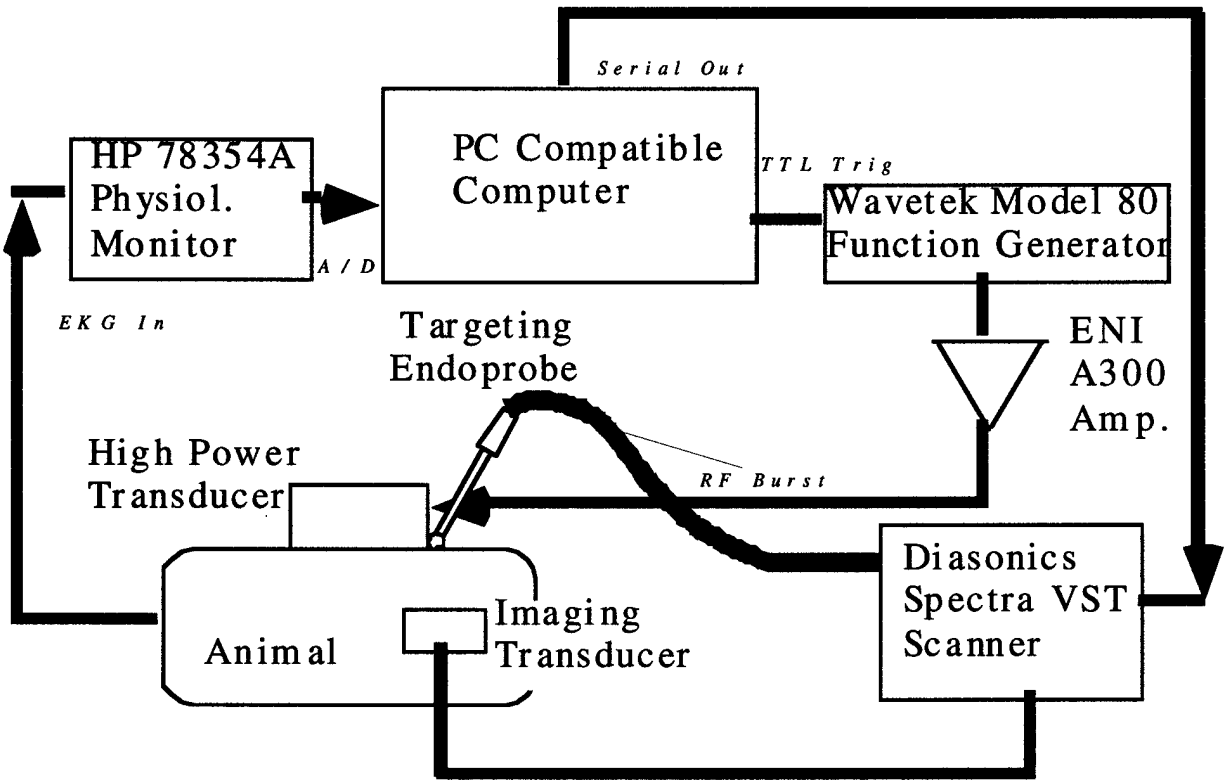
Serial Out
HP 78354A
Physiol.
Monitor
A / D
PC Compatible
Computer
TTL Trig
Wavetek Model 80
Function Generator
EKG In
Targeting
Endoprobe
ENI
A300
Amp.
High Power
Transducer
RF Burst
Diasonics
Spectra VST
Scanner
Animal
Imaging
Transducer

**Figure 1**

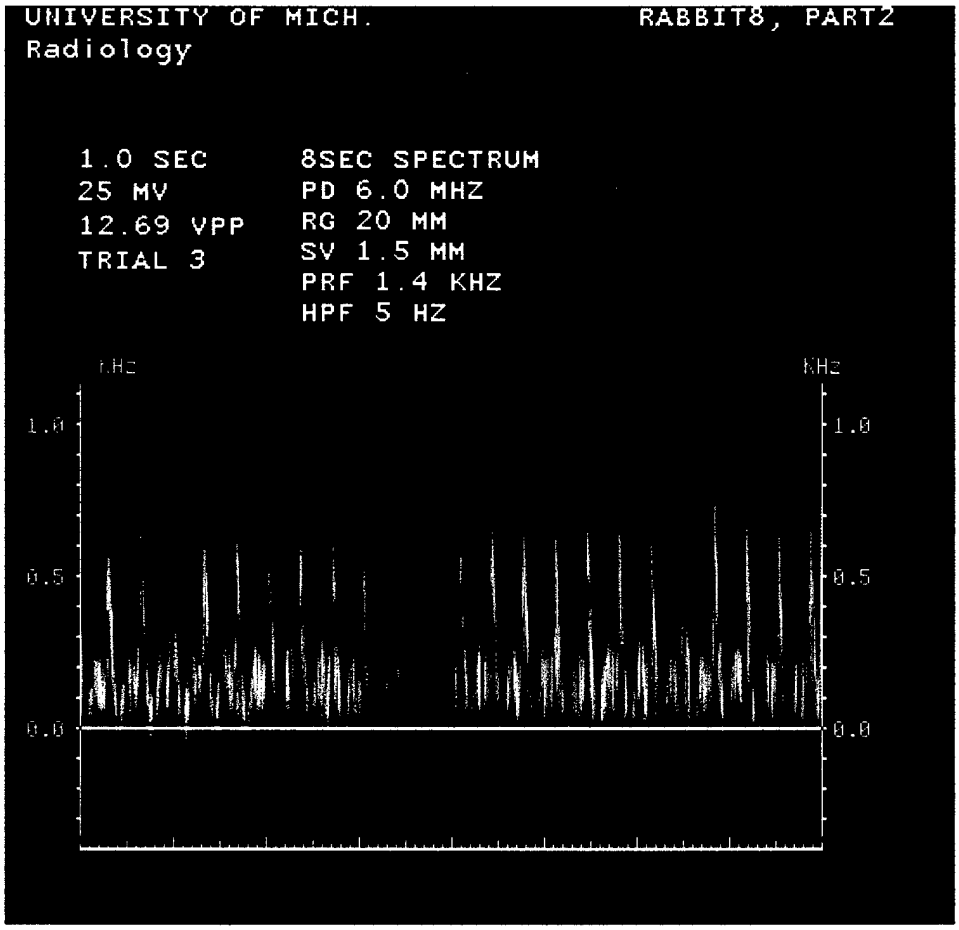


Figure 2A

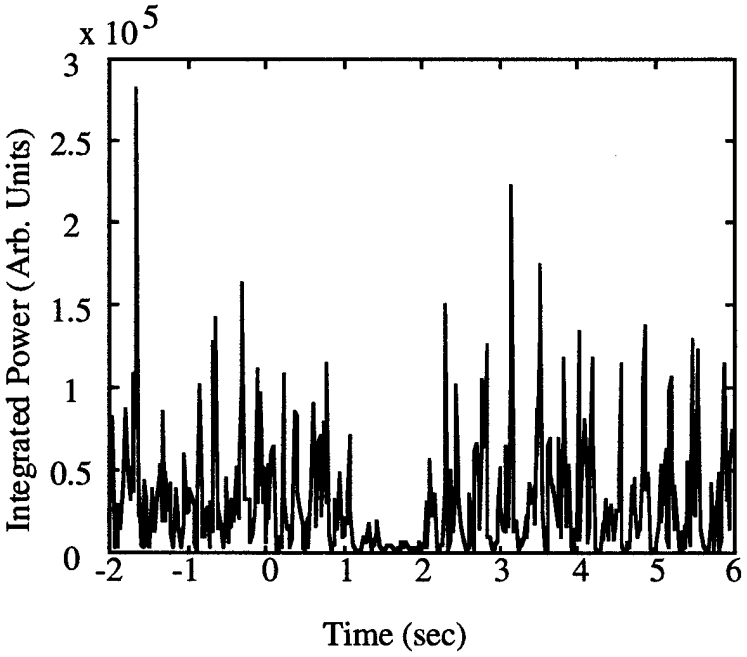


Figure 2B

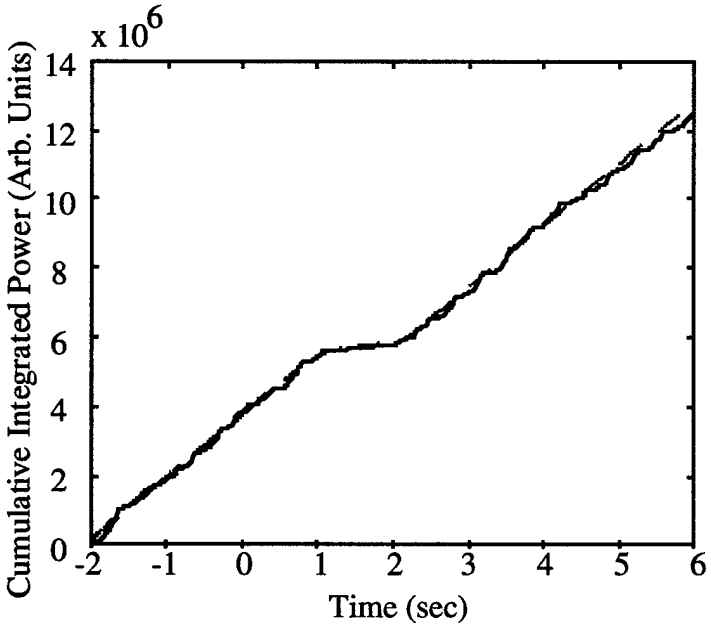


Figure 2C

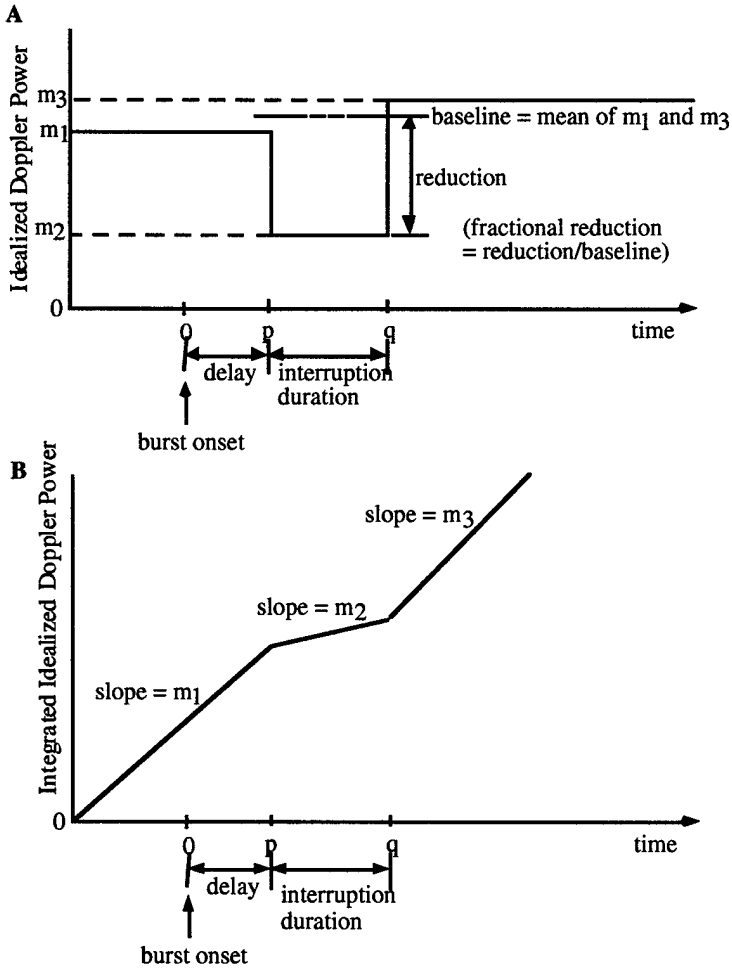


Figure 3

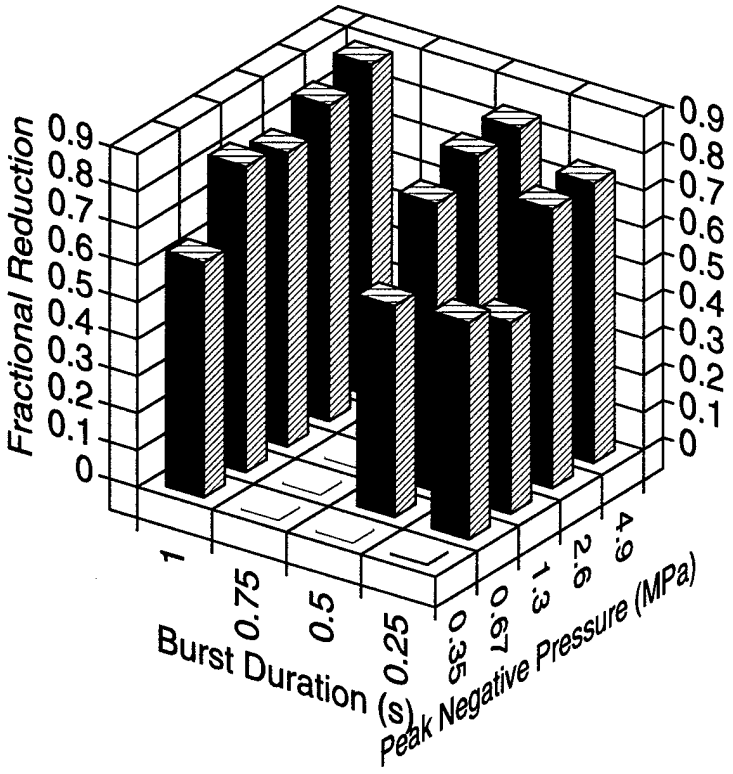


Figure 4A

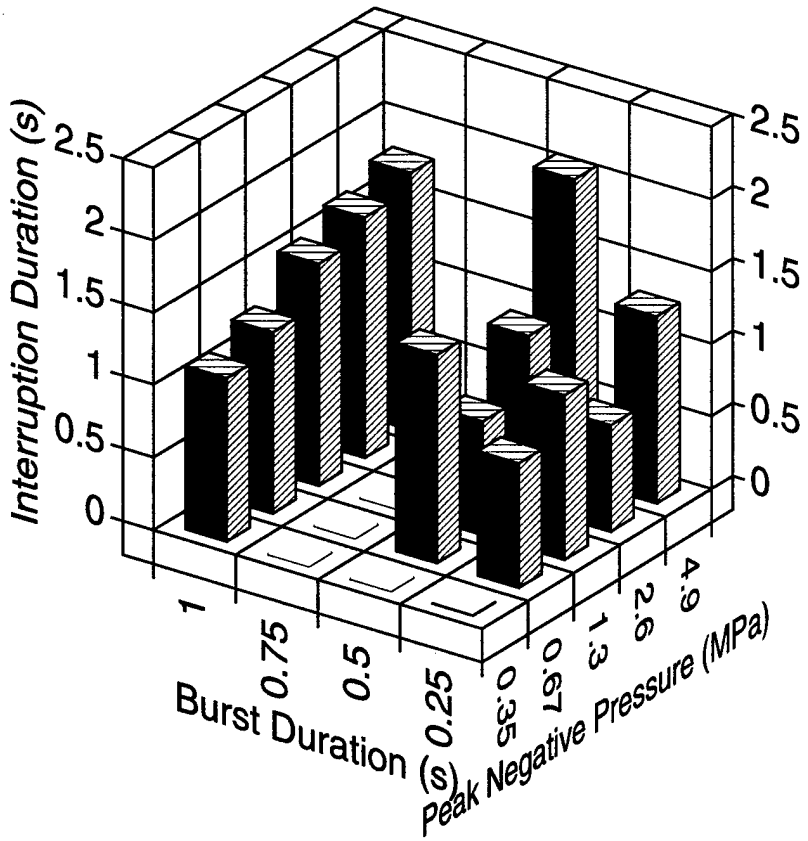


Figure 4B

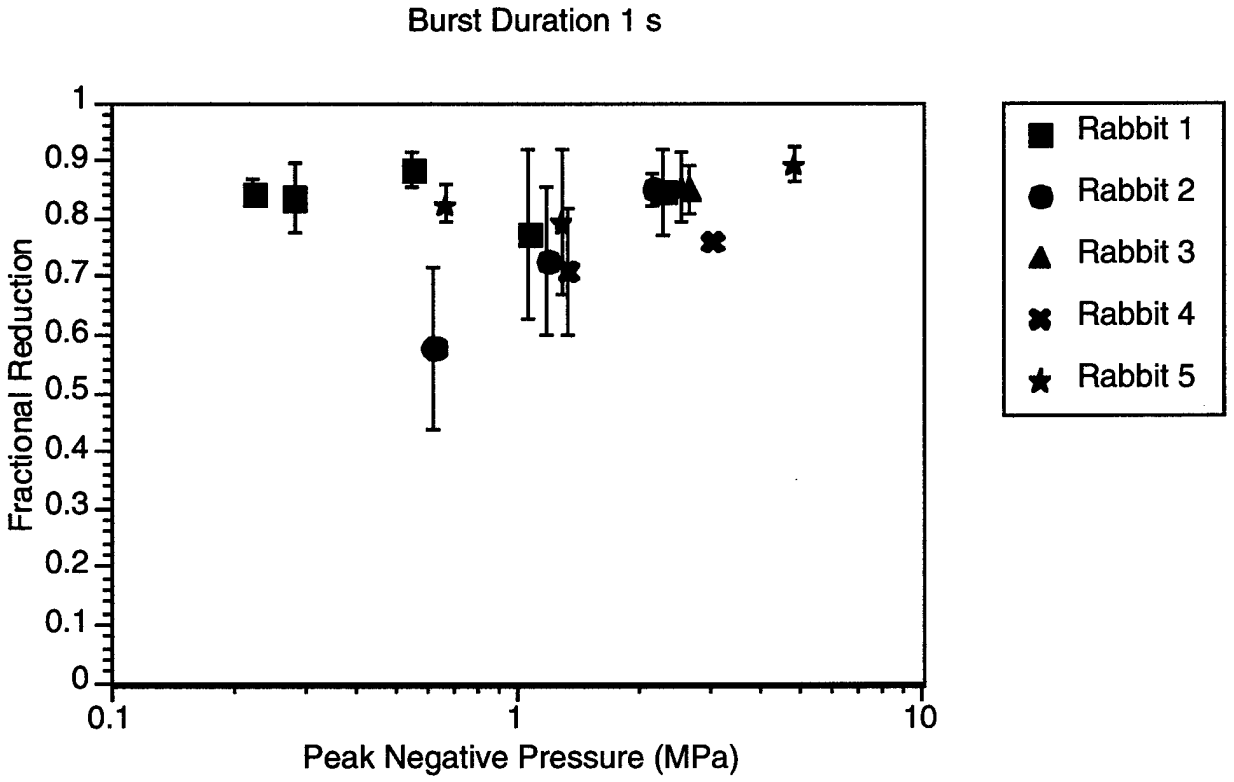


Figure 5A

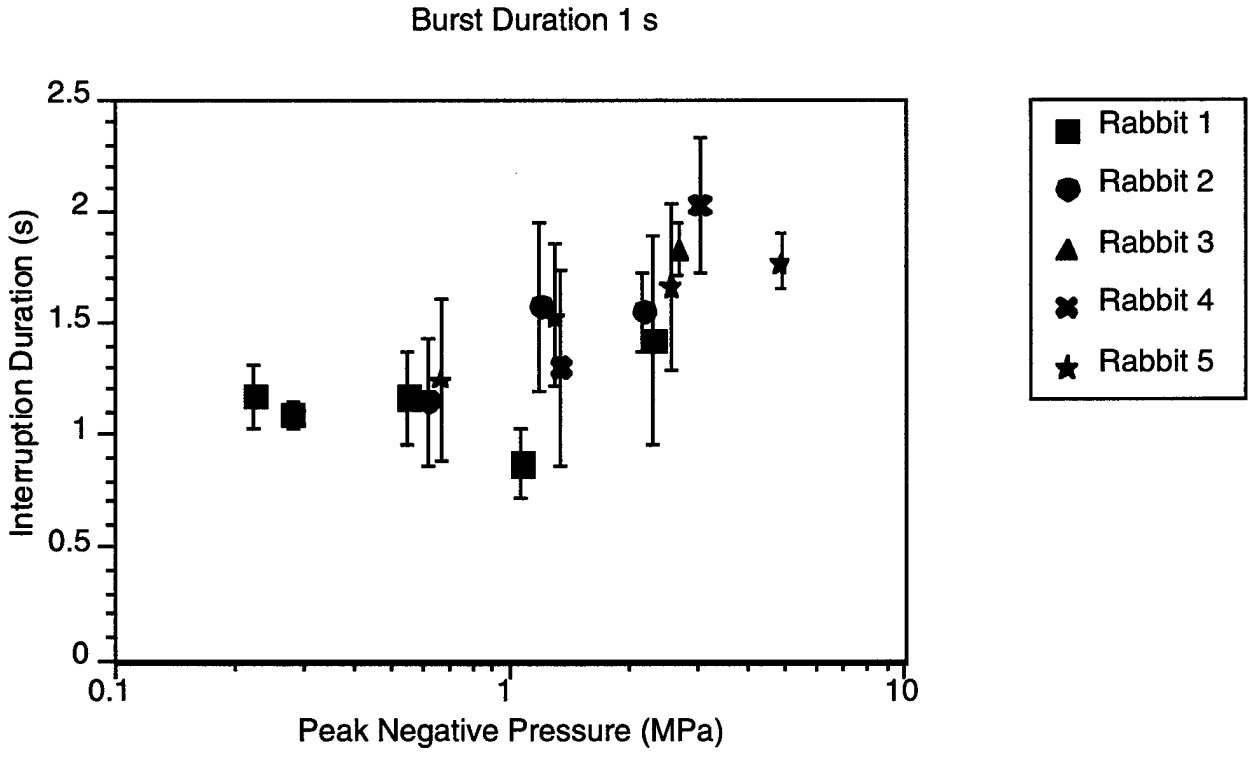


Figure 5B

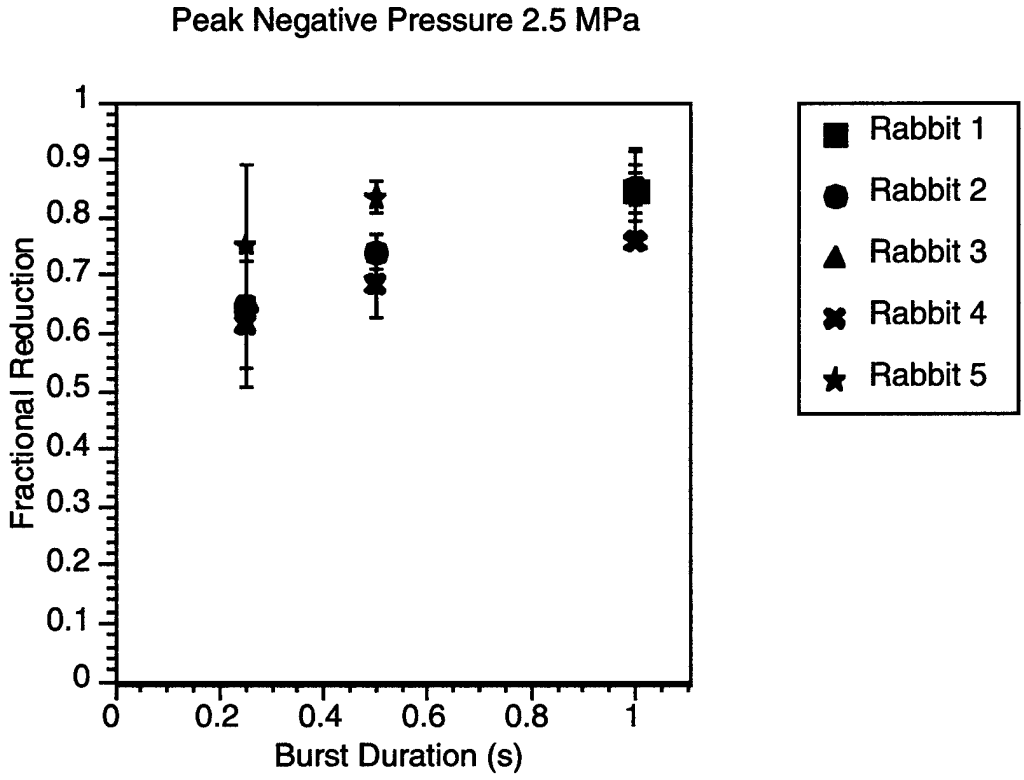


Figure 5C

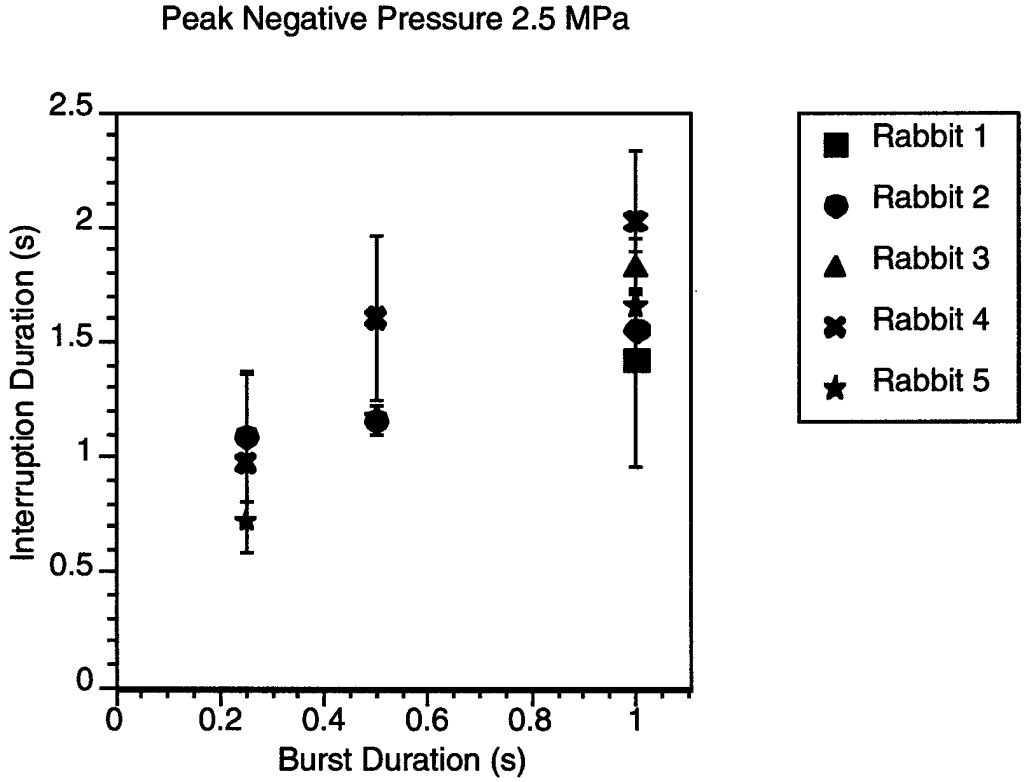


Figure 5D

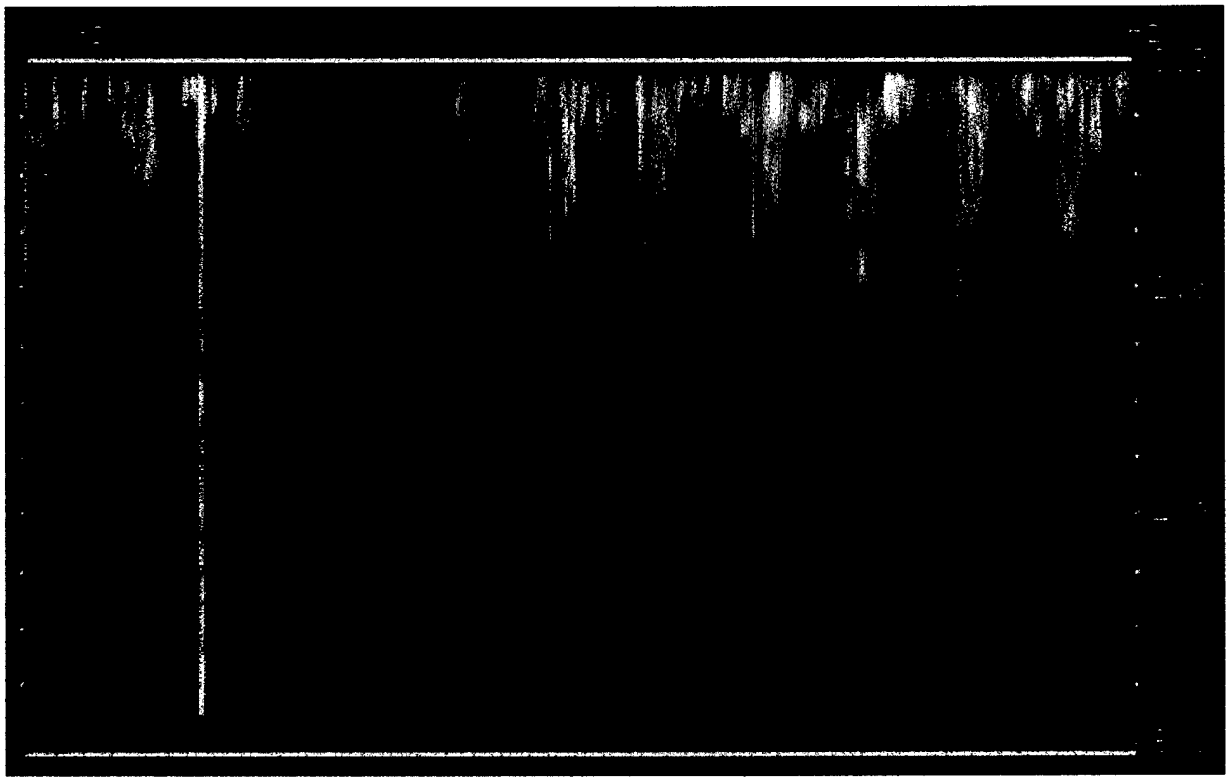

Figure 6A

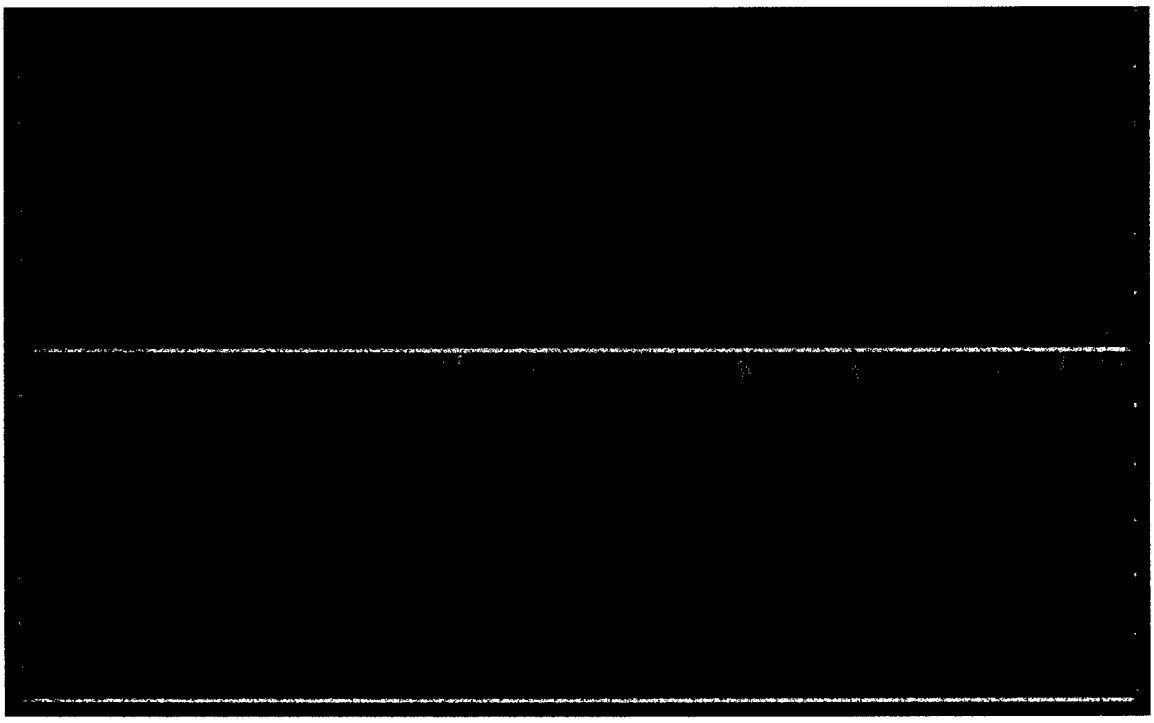

Figure 6B

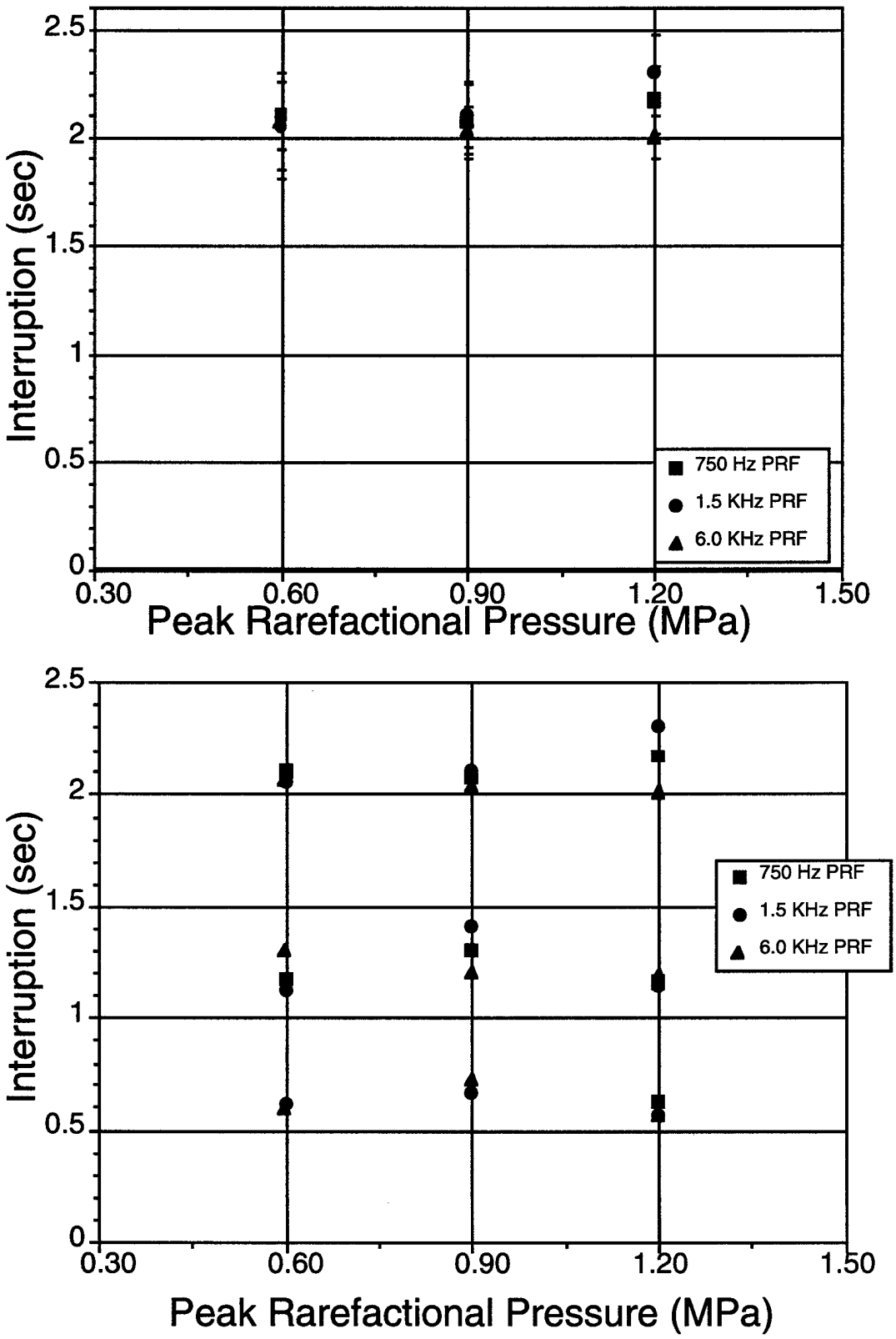


Figure 7A (top) and 7B (bottom)

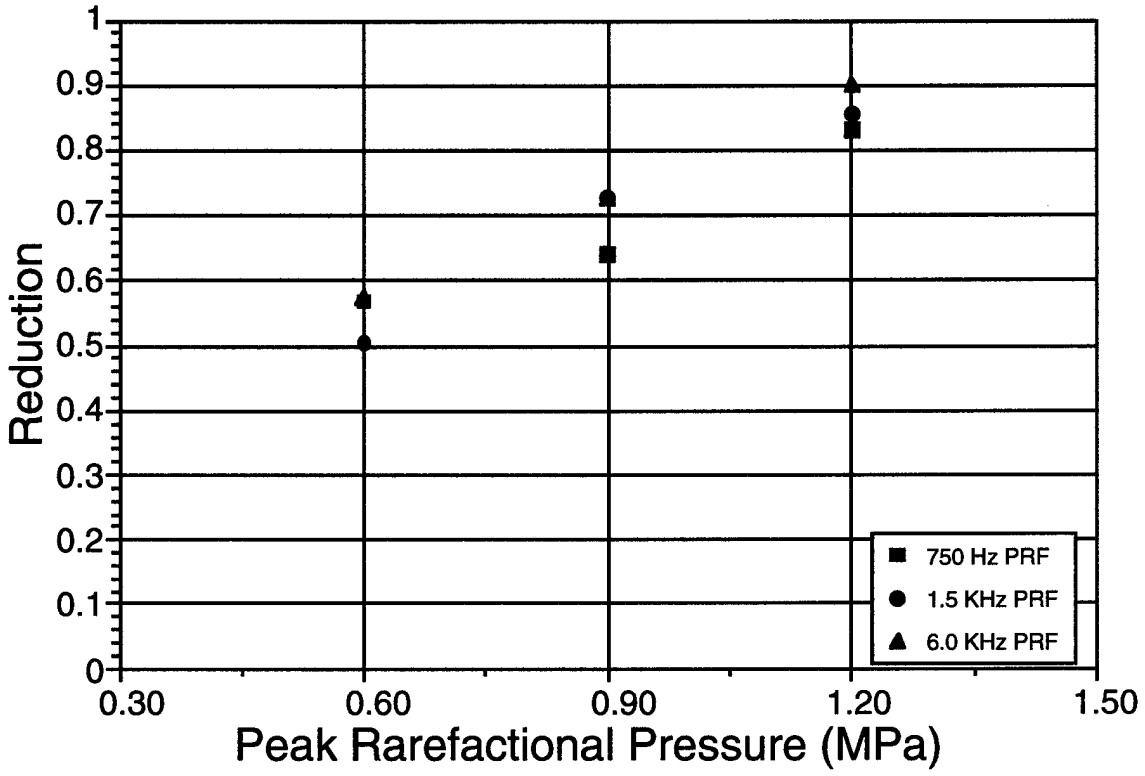


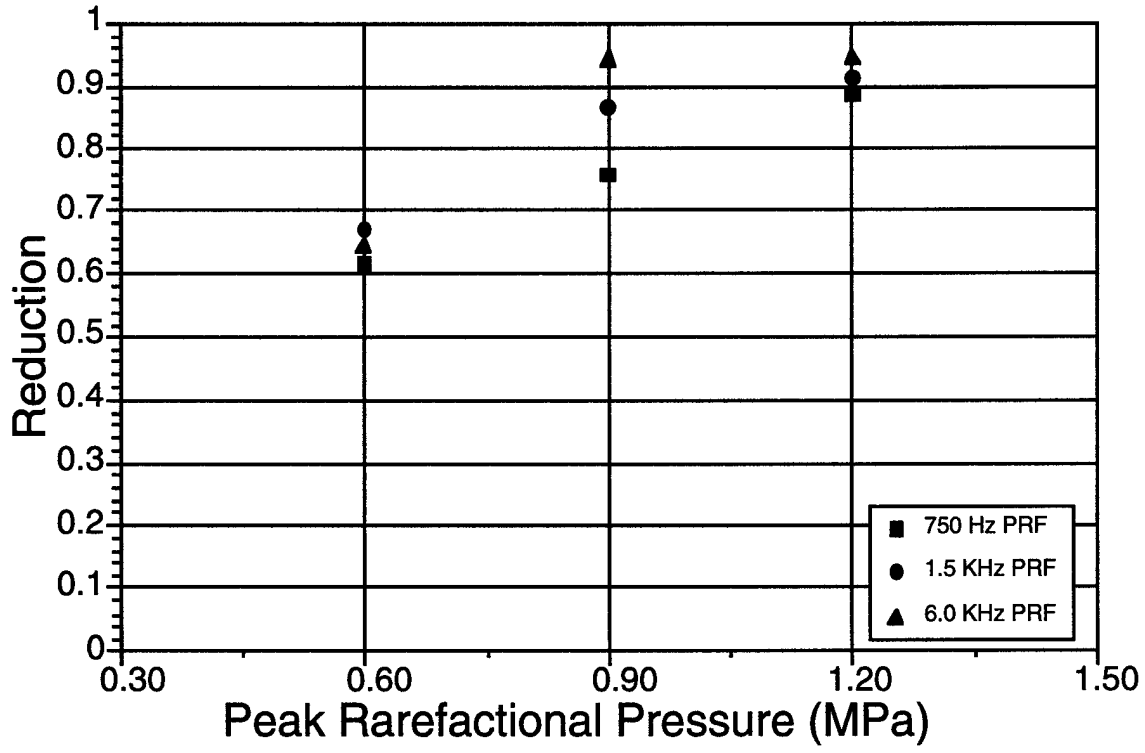


Figure 8A (top) and 8B (bottom)

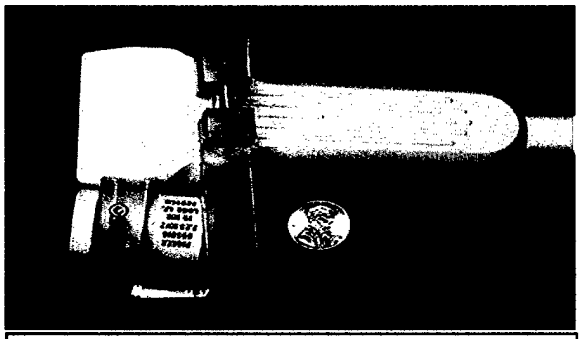

Figure 9

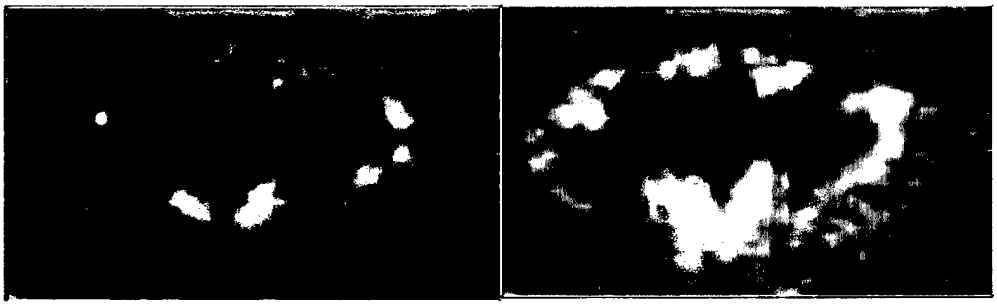

Figure 10

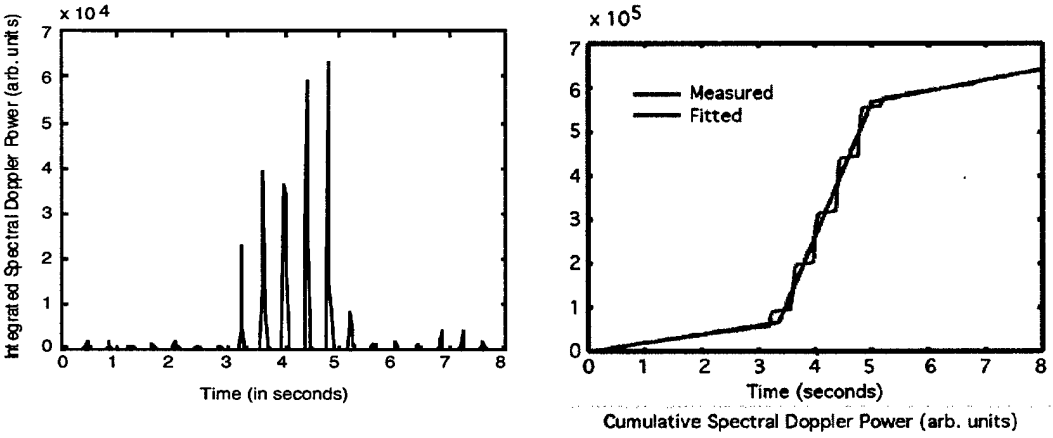


**Figure 11**

A B

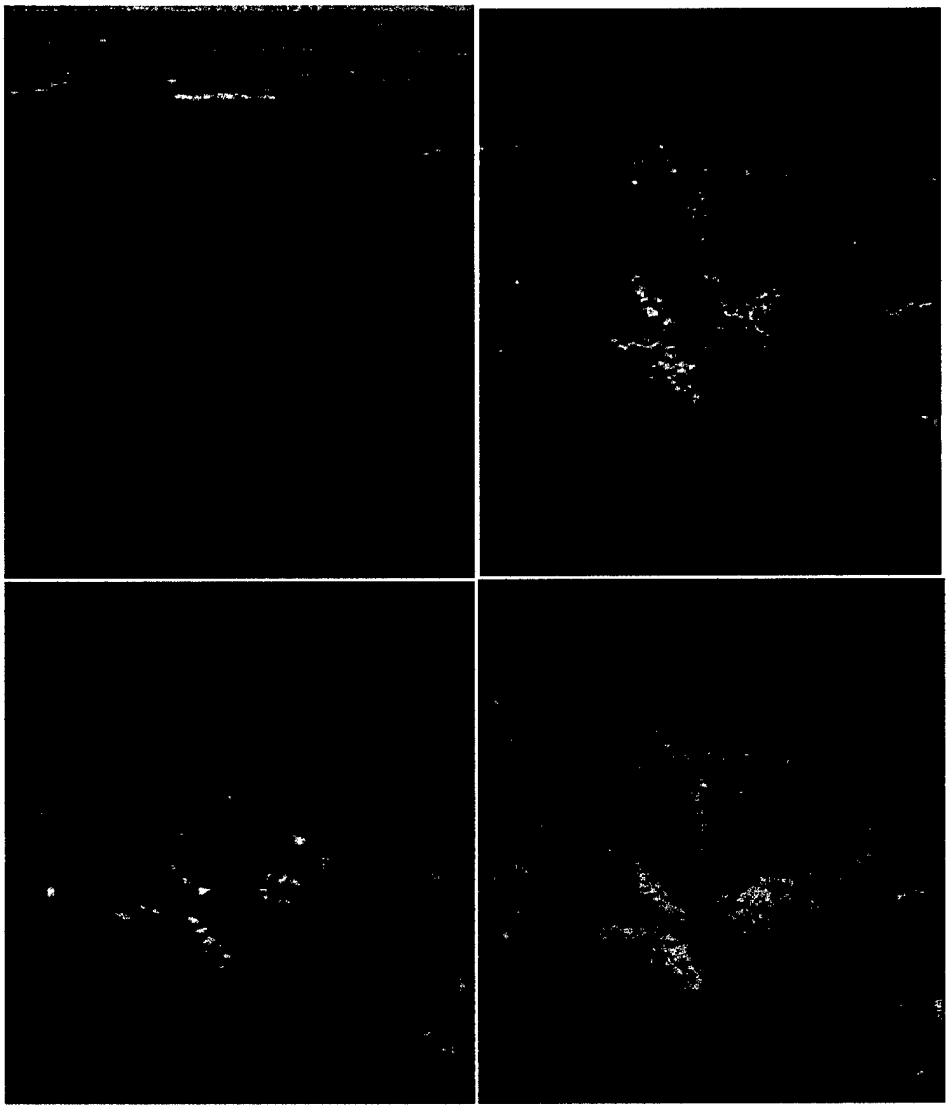

C D

**Figure 12**

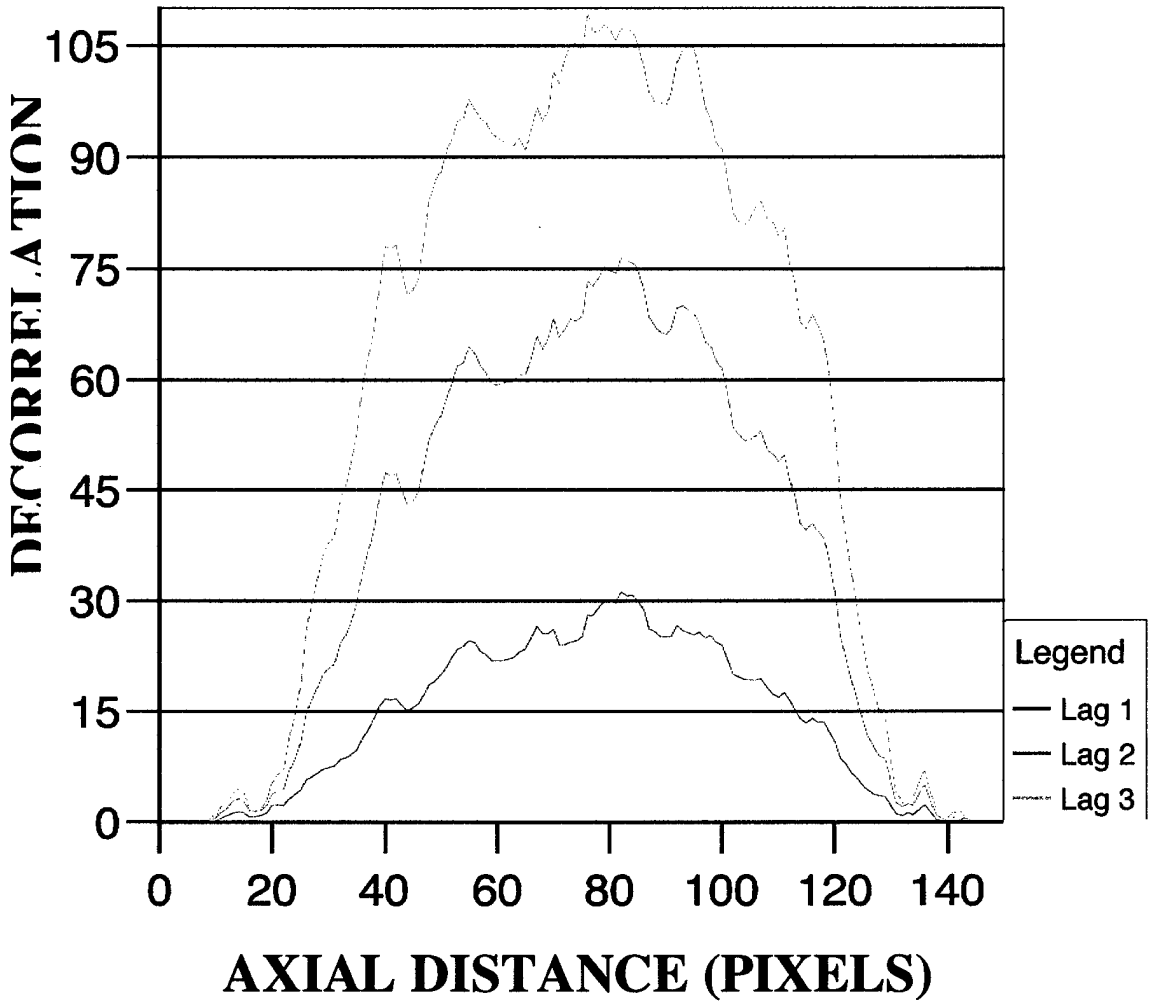
DECORRELATION OF TUBE FLOW
MEAN FLOW VELOCITY = 0.483 CM/SEC
DECORRELATION
105
90
75
60
45
30
15
0
0
20
40
60
80
100
120
140
AXIAL DISTANCE (PIXELS)
Legend
Lag 1
Lag 2
Lag 3

**Figure 13a**

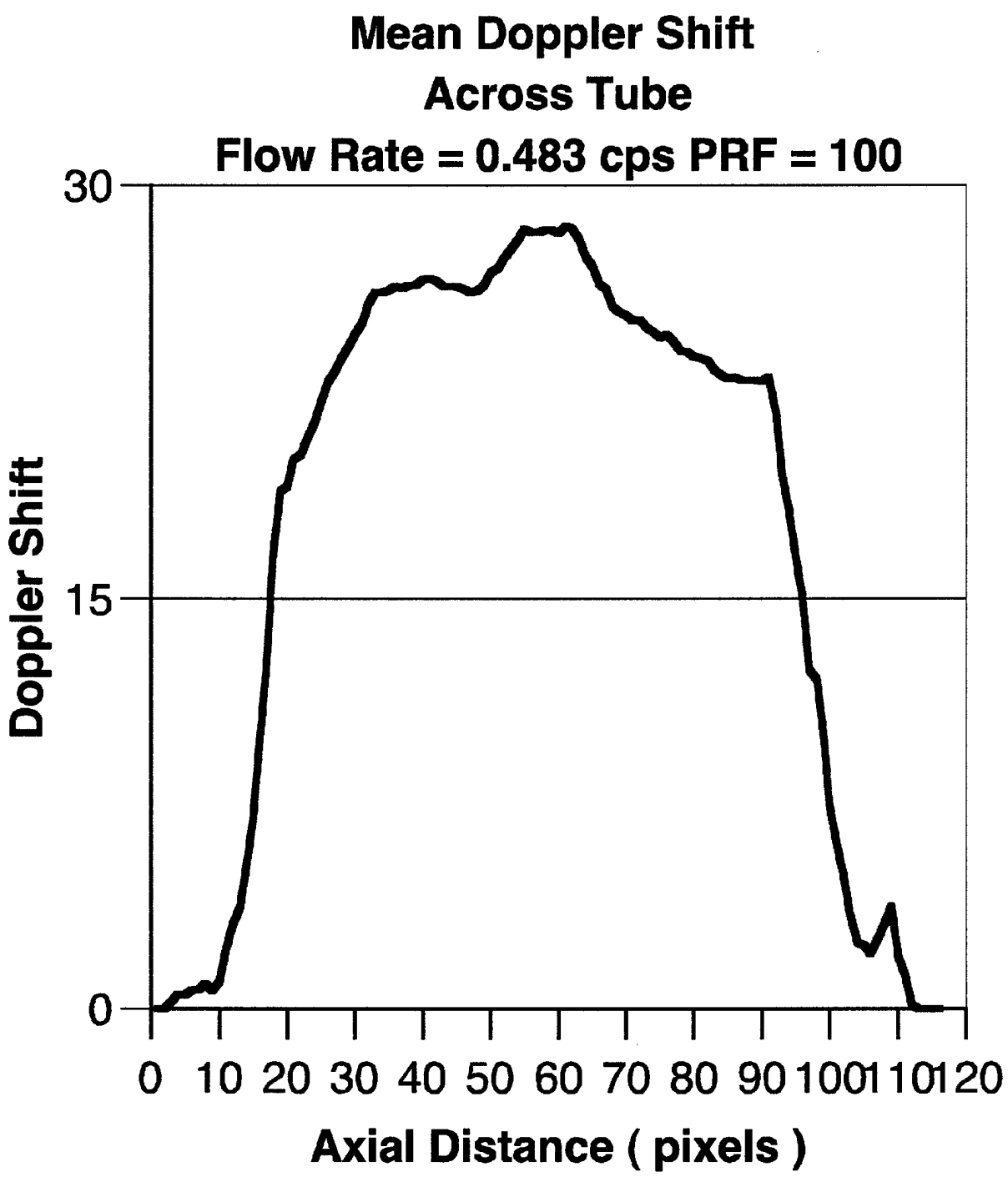
Mean Doppler Shift
Across Tube
Flow Rate = 0.483 cps PRF = 100
Doppler Shift
30
15
0
0 10 20 30 40 50 60 70 80 90 100 110 120
Axial Distance ( pixels )

**Figure 13b**

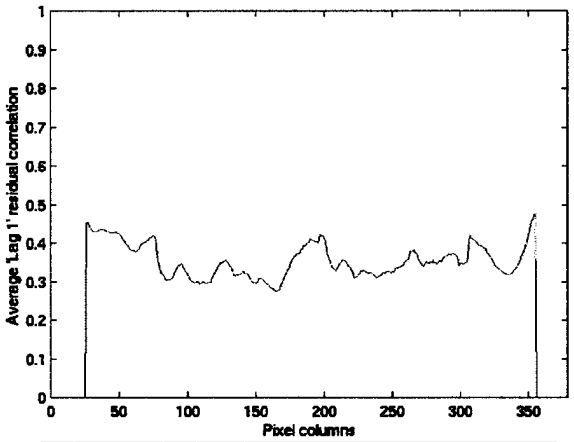


**Figure 14**

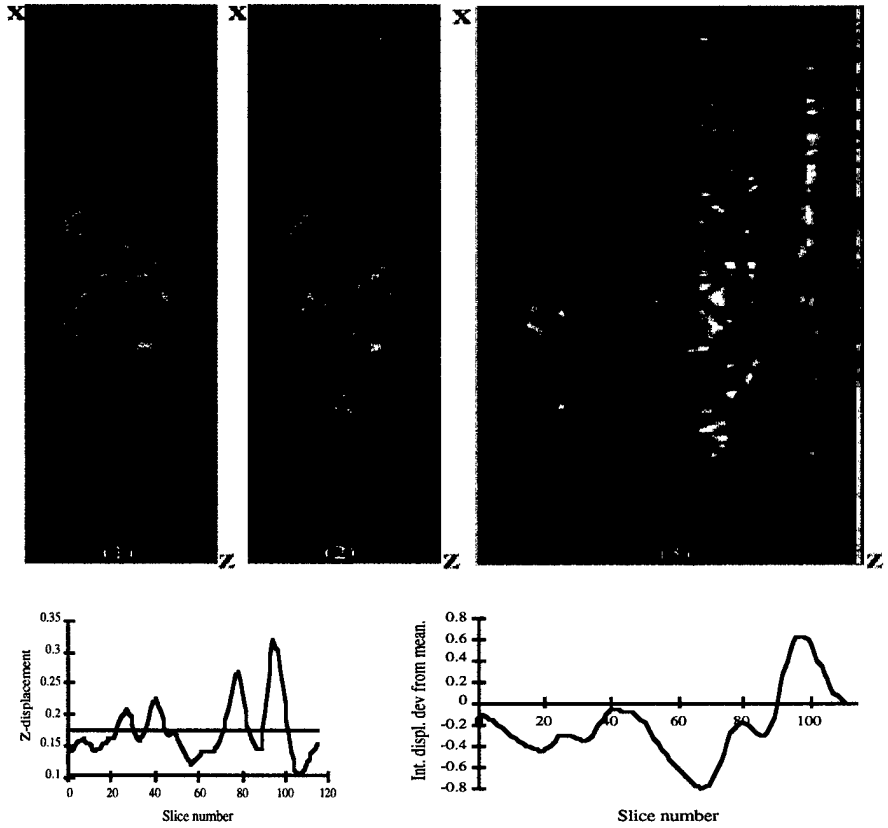


**Figure 15**

**Figure 16**

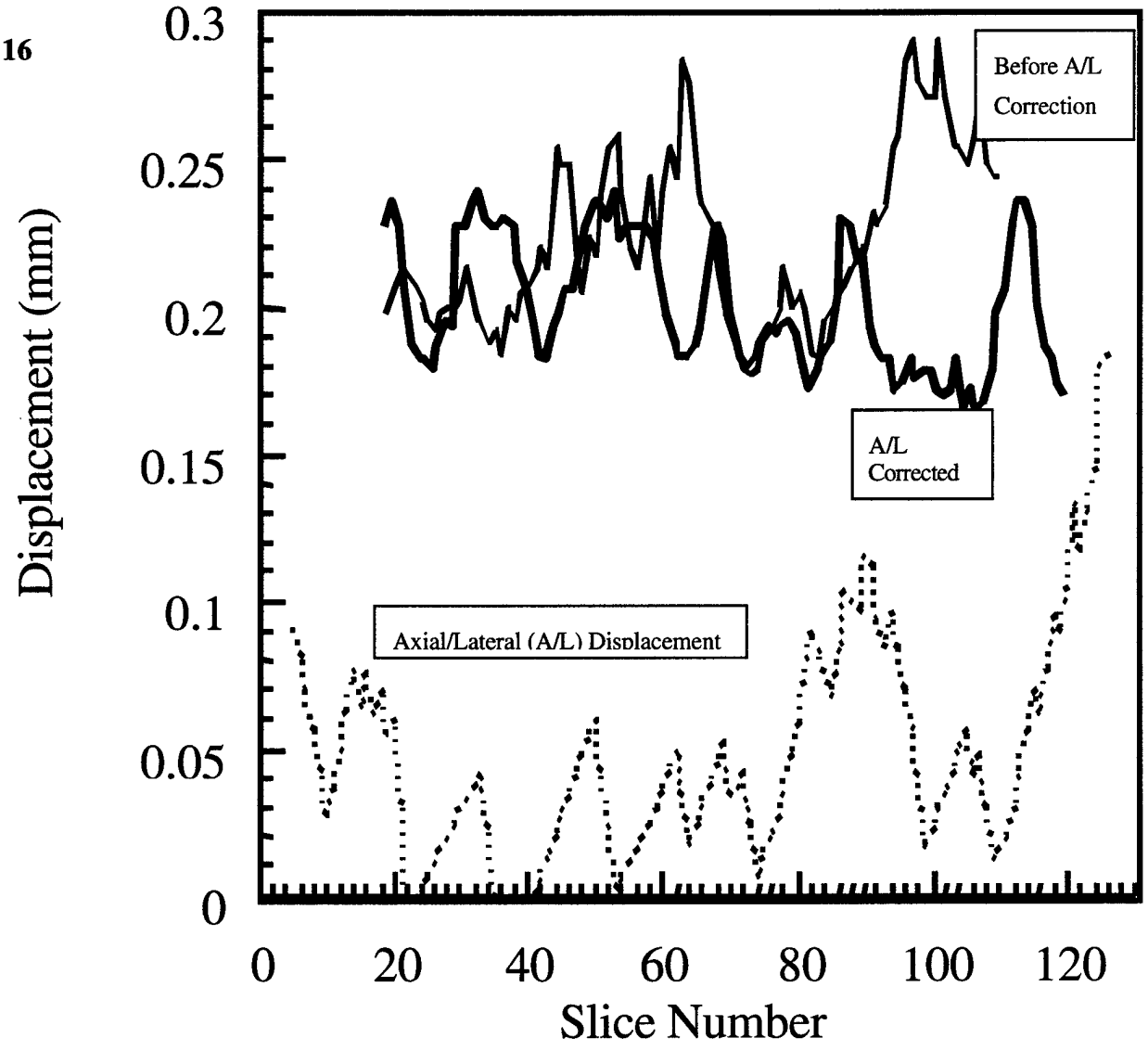
Displacement (mm)
0.3
0.25
0.2
0.15
0.1
0.05
0
0
20
40
60
80
100
120
Slice Number
Before A/L Correction
A/L Corrected
Axial/Lateral (A/L) Displacement